


RESEARCH

Open Access



Clinical recovery of *Macaca fascicularis* infected with *Plasmodium knowlesi*

Mariko S. Peterson^{1,2,15†}, Chester J. Joyner^{1,2,3,16†} , Jessica A. Brady^{4,17}, Jennifer S. Wood⁵, Monica Cabrera-Mora^{1,2,18}, Celia L. Saney^{1,2}, Luis L. Fonseca^{6,19}, Wayne T. Cheng³, Jianlin Jiang^{1,2}, Stacey A. Lapp^{1,2}, Stephanie R. Soderberg^{1,2,20}, Mustafa V. Nural⁷, Jay C. Humphrey^{7,21}, Allison Hankus^{1,2,22}, Deepa Machiah⁸, Ebru Karpuzoglu^{1,2,23}, Jeremy D. DeBarry^{7,24}, MaHPIC-Consortium, Rabindra Tirouvanziam⁹, Jessica C. Kissinger^{7,10,11}, Alberto Moreno^{1,2,12}, Sanjeev Gumber^{8,13,25}, Eberhard O. Voit⁶, Juan B. Gutiérrez^{14,26}, Regina Joice Cordy^{1,2,27} and Mary R. Galinski^{1,2,12*}

Abstract

Background: Kra monkeys (*Macaca fascicularis*), a natural host of *Plasmodium knowlesi*, control parasitaemia caused by this parasite species and escape death without treatment. Knowledge of the disease progression and resilience in kra monkeys will aid the effective use of this species to study mechanisms of resilience to malaria. This longitudinal study aimed to define clinical, physiological and pathological changes in kra monkeys infected with *P. knowlesi*, which could explain their resilient phenotype.

Methods: Kra monkeys ($n = 15$, male, young adults) were infected intravenously with cryopreserved *P. knowlesi* sporozoites and the resulting parasitaemias were monitored daily. Complete blood counts, reticulocyte counts, blood chemistry and physiological telemetry data ($n = 7$) were acquired as described prior to infection to establish baseline values and then daily after inoculation for up to 50 days. Bone marrow aspirates, plasma samples, and 22 tissue samples were collected at specific time points to evaluate longitudinal clinical, physiological and pathological effects of *P. knowlesi* infections during acute and chronic infections.

Results: As expected, the kra monkeys controlled acute infections and remained with low-level, persistent parasitaemias without anti-malarial intervention. Unexpectedly, early in the infection, fevers developed, which ultimately returned to baseline, as well as mild to moderate thrombocytopenia, and moderate to severe anaemia. Mathematical modelling and the reticulocyte production index indicated that the anaemia was largely due to the removal of uninfected erythrocytes and not impaired production of erythrocytes. Mild tissue damage was observed, and tissue parasite load was associated with tissue damage even though parasite accumulation in the tissues was generally low.

Conclusions: Kra monkeys experimentally infected with *P. knowlesi* sporozoites presented with multiple clinical signs of malaria that varied in severity among individuals. Overall, the animals shared common mechanisms of resilience characterized by controlling parasitaemia 3–5 days after patency, and controlling fever, coupled with physiological and bone marrow responses to compensate for anaemia. Together, these responses likely minimized tissue damage while supporting the establishment of chronic infections, which may be important for transmission in natural

*Correspondence: Mary.Galinski@emory.edu

†Mariko S. Peterson and Chester J. Joyner contributed equally to this work

¹ Yerkes National Primate Research Center, Emory University, Atlanta, GA, USA

Full list of author information is available at the end of the article



endemic settings. These results provide new foundational insights into malaria pathogenesis and resilience in kra monkeys, which may improve understanding of human infections.

Keywords: Malaria, Nonhuman primate models, Cynomolgus monkeys, Infectious diseases resilience, Telemetry, Fever, Anaemia, Thrombocytopenia, Bone marrow, Histopathology

Background

Plasmodium knowlesi malaria cases have been identified in 10 of the 11 countries that comprise Southeast Asia; the one exception being Timor-Leste (reviewed in [1–3]). Since its recognition in 2004 in Malaysia as an emergent zoonotic parasite species [4], *P. knowlesi* has in fact risen as the major cause of human clinical cases of malaria in Malaysia and threatens to upend malaria elimination in this country [1, 2, 4–8]; over 4000 Malaysian cases of *P. knowlesi* malaria were reported in 2018 [9]. *Plasmodium knowlesi* transmission to humans has been attributed to spillover events from peri-domestic infected macaques in village settings, or from infected wild macaques in the setting of jungle trekking, foraging, farming, and logging activities [1, 5, 10–13]. At least three macaque species are endemic to these geographical regions and can serve as reservoirs for *P. knowlesi*: *Macaca fascicularis* (the kra monkey, also known as cynomolgus monkey or long-tailed macaque), *Macaca nemestrina* (pig-tailed macaque) and *Macaca arctoides* (stump-tailed macaque) [14–17].

Plasmodium knowlesi infections cause symptoms that are generally associated with malaria caused by other *Plasmodium* species (*Plasmodium falciparum*, *Plasmodium vivax*, *Plasmodium malariae*, and *Plasmodium ovale*, and the closely related zoonotic species *Plasmodium cynomolgi*) [18–21], including cyclical episodes of fever and chills with rigor. Clinical complications have the potential to become exacerbated quickly given this species' unique 24-h replication cycle within the erythrocyte host cell [1, 5, 22–24]. Asymptomatic *P. knowlesi* infections are also common [25–29], including a high percentage in children [12]. Clinically, thrombocytopenia has been reported as a universal problem with *P. knowlesi* infections (< 150,000 platelets/ml), with about 1/3 of adult patients showing severe thrombocytopenia (< 50,000 platelets/ml) [reviewed in 1]. Anaemia is not a predominant problem with *P. knowlesi* malaria in adults, though moderate anaemia (defined as less than 10 g/dl) and recovery from this disease state have been observed, and some cases of severe anaemia (less than 7 g/dl) have been documented [24, 30] and reviewed in [1]. In contrast, anaemia has been identified as a predominant feature in children with *P. knowlesi* malaria [31], despite children having lower parasitaemias (and no fatalities reported) [32]. While hyperparasitaemia is associated

with severe disease, it should be noted that *P. knowlesi* can cause clinical manifestations at lower parasitaemias than other species (e.g., baseline median values on hospital admission in Kapit of 1387 *P. knowlesi* parasites/ml, compared to 4258 *P. vivax* parasites/ml and 26,781 *P. falciparum* parasites/ml) [24]. Also, Barber and others showed in a prospective study that in Sabah, Malaysia, *P. knowlesi* was more likely than *P. falciparum* to cause severe disease [30].

In severe cases of *P. knowlesi* malaria, clinical signs and symptoms in adults have included abdominal pain, shortness of breath, productive cough, and respiratory distress [1, 6, 23, 24]. Severe cases have included jaundice, acute kidney injury, metabolic acidosis, acute lung injury, and shock, among others [reviewed in 33, 34]. High parasitaemia (> 20,000 *P. knowlesi* parasites/ml) along with jaundice and thrombocytopenia have been identified as putative indicators for severe disease [1, 24, 30]. Cerebral malaria and coma have not been associated with *P. knowlesi*, although severe malaria including hyperparasitaemia can result in cerebral pathology as shown in one reported autopsy case of *P. knowlesi* [23].

Daneshvar et al. reported close to 10% of hospital cases of *P. knowlesi* malaria with severe complications and a case fatality rate in their study of 1.8% [24] while others have reported higher numbers for severe cases (29% and 39% of hospital cases studied) [30, 35] and deaths (six deaths out of 22 patients with a severe case of *P. knowlesi* malaria) [35]. As of 2017, 41 deaths were reported in Malaysia [36]. Notably, deaths are being averted in recent years with improved monitoring and diagnosis and the timely use of intravenous artesunate [37] or artemisinin-based combination therapy (ACT) [30, 33, 38, 39].

As this zoonotic disease remains prevalent, gaining an improved understanding of the pathogenesis of *P. knowlesi* is important. Such an understanding can be gained with the use of nonhuman primate (NHP) models (reviewed in [40–42]). Experimental infections can be designed that consider the infecting parasite species and genotype(s), the parasite stage and size of the inoculum, the duration of infections through acute and chronic stages of illness, experimental interventions, treatments, and the immune status of the host. Furthermore, tissue samples can be collected at selected times for pathology studies.

Multiple NHP species can be experimentally infected with *P. knowlesi* (reviewed in [40, 41, 43]). The most

explored have been rhesus and kra monkeys. Malaria-naïve rhesus macaques will invariably succumb to *P. knowlesi* infection, unless treated with anti-malarial drugs, because of the unceasing, overwhelming rise in parasitaemia and the continued cyclical destruction of erythrocytes that occurs unabated in this species with the multiplication of the parasites every 24 h [43–48]. Thus, rhesus macaques are viable animal models for severe disease due to hyperparasitaemia. In the course of ~ 50 years, rhesus monkey infections became the main experimental host to study *P. knowlesi* biology, virulence, immune responses, antigenic variation and pathology, with much knowledge yet to be uncovered in each of these areas (e.g., see [46–50]) and (reviewed in [41, 42]). In stark contrast, malaria-naïve kra monkeys are able to control parasitaemia without anti-malarial treatment, typically with a maximum of 1–3% parasitaemia [43–45, 51, 52], making them the preferred animal model for mild, moderate or chronic *P. knowlesi* malaria.

Despite the potential of kra monkeys for revealing mechanisms of resilience to *P. knowlesi* infections, only a few small studies have so far reported features of *P. knowlesi* infections and pathology in kra monkeys [53, 54]. Anderios et al. reported haematological and liver and spleen histopathology data from two kra monkeys after 60 or 90 days of infection post-inoculation either with *P. knowlesi*-infected blood from a patient or cryopreserved *P. knowlesi* (Malayan strain)-infected rhesus blood [53]. Barber et al. studied the deformability of RBCs from both *P. knowlesi*-infected patients and three infected kra monkeys [54]. In-depth longitudinal characterizations of clinical and other parameters during the course of *P. knowlesi* acute and chronic infections in this resilient host species and tissue pathology analysis will complement clinical investigations and therapeutic considerations.

By combining telemetric, clinical, parasitological and pathological data, collected longitudinally for up to 50 days, the present investigation demonstrates that kra monkeys develop and recover without treatment from clinical manifestations of malaria, including fever, thrombocytopenia and anaemia. Low parasitaemias, low parasite tissue burdens, and overall mild tissue damage and organ dysfunction define this resilient phenotype. By highlighting the clinical and pathological consequences of *P. knowlesi*, this study provides a framework for basic and systems biological studies utilizing the *P. knowlesi*-kra monkey model for studying malaria resilience and pathogenesis [55]. Possible systemic mechanisms and potential research directions are discussed to better understand these phenomena and consider future novel therapies.

Methods

Animal use and approvals

Experiments involving NHPs were performed at the Yerkes National Primate Research Center (YNPRC), an AAALAC International-accredited facility, following ARRIVE Guidelines and Recommendations [56]. All experimental, surgical, and necropsy procedures were approved by Emory's IACUC and the Animal Care and Use Review Office (ACURO) of the US Department of Defense and followed accordingly. The Emory's IACUC approval number was PROTO201700484-YER-2003344-ENTRPR-A. Fifteen *M. fascicularis* (Mauritius origin, born and raised at the Mannheimer Foundation, Inc., Homestead, FL, USA), all healthy and malaria-naïve young adults (3–5 years old) were assigned within three cohorts for sequential longitudinal systems biology infection experiments, primarily aiming to study both acute and chronic phases of infection and to understand the resilience phenotype exhibited by *M. fascicularis* with *P. knowlesi* blood-stage infections. The majority of the kra monkeys were not consanguineous. All had different dams and the majority had different sires, except for the following: H12C59 and H14C17 had two same potential sires and 14C3 and 14C15 had two potential same sires. Euthanasia and necropsies were performed at selected times to analyze tissue data from animals at acute (n = 4) and chronic (n = 11) phases of infection (Additional file 1: Table S1 and Additional file 10: Fig. S1, Additional file 11: Fig. S2, Additional file 12: Fig. S3). Male monkeys were selected to eliminate confounding anaemia measurements due to menstruation. All animals were housed socially, with 12-h light–dark cycles, in housing compliant with the Animal Welfare Act and the Guide for the Care and Use of Laboratory Animals. Environmental enrichment consisting of food and physical manipulanda was provided daily. The animals received positive reinforcement training to habituate them to ear-stick blood collections for blood smear preparations and clinical analyses requiring blood collections of less than 150 µl. The weight of the animals was determined to be between 5.6 kg and 11.7 kg at the endpoint of each experiment, when necropsies and tissue analyses were performed. The animals were anaesthetized using ketamine and euthanized via intravenous administrations of barbiturates. This euthanasia method is an acceptable method of euthanasia for NHPs per the recommendations of the “AVMA Guidelines for the Euthanasia of Animals”.

Parasite isolates and inoculations

The monkeys from experimental cohorts E07, E33 and E35 (Additional file 1: Table S1) were infected

intravenously with ~ 100,000 cryopreserved *P. knowlesi* clone Pk1(A+) sporozoites derived from the Malayan strain of *P. knowlesi* [57] (kindly provided by John W. Barnwell, Centers for Disease Control and Prevention, Atlanta, GA), which had been suspended in RPMI 1640 with 50% fetal calf serum and quick frozen, and when thawed estimated to be 0.1–1% viable; John W. Barnwell, personal communication). The Experiment 07 cohort was initially inoculated with sporozoites freshly dissected from mosquitoes at the Centers for Disease Control and Prevention, but for unexplained reasons parasitaemia did not develop in the blood. The E07 cohort was subsequently inoculated (about 80 days later) with the same batch of cryopreserved sporozoites used to infect the two other cohorts. There was no evidence that the animals had developed immunity based on similar infection kinetics across the cohorts, and significant differences were not detected in the repeated baseline transcripts [55]. Tissues from normal uninfected animals from E34 (Additional file 1: Table S1), as well as archived tissue blocks from the YNPRC tissue repository, were used as negative controls for histopathological comparisons.

Sample collections

Bone marrow (BM) aspirates from the iliac crest and venous blood collections were collected into EDTA. Capillary blood samples were collected into EDTA using standardized ear-stick procedures for complete blood counts (CBCs) and monitoring of parasitaemia.

Telemetry

The monkeys in the E07 cohort ($n = 7$) had telemetry devices surgically implanted about 4–5 weeks prior to the initial inoculation of sporozoites, for real-time monitoring of temperature and other vital signs (Brady et al., manuscript in preparation). The devices were activated to collect continuous telemetry data about 2 weeks prior to the inoculation of sporozoites (see Additional file 1: Table S1 and Additional file 10: Fig. S1). These devices were not included in the experimental design of the E33 and E35 protocols, which comprised two iterative studies without these measurements among the goals. In brief, the PhysioTel™ L11 telemetry implant device was secured between the external and internal abdominal oblique muscles. Raw temperature data, used in the current study, was obtained with a 1 Hz sampling frequency after which missing value indicators were removed. Hourly temperature averages were obtained using a subset of the data, minute averages obtained from the first 15 s of each minute if available, and then smoothed using

the Hodrick-Prescott filter to reduce noise. The normal temperature range for each monkey was defined as the range of temperatures measured prior to inoculation of *P. knowlesi* sporozoites. The febrile threshold was determined by considering the parasitaemia prior to the time when the temperature rose above the individual's threshold. The time-to-temperature response was determined as the day post-inoculation when the temperature rose above the individual's threshold.

Quantification of reticulocyte production index

Reticulocyte production index (RPI) was calculated to assess bone marrow responsiveness to anaemia, and is given by the following equation, as described previously [58]:

$$RPI = \frac{\text{Percent peripheral reticulocytes}}{\text{Reticulocyte maturation}} \times \frac{\text{Haemoglobin}}{\text{Individual baseline haemoglobin}}$$

Parasite enumeration

Parasitaemia was enumerated daily between 1 and 3 PM when synchronous ring-stage parasites predominated until the infections became patent. After patency, twice-daily capillary samples (8 AM, schizonts; and 1–3 PM ring stages) were acquired for parasitaemia monitoring. Thick and thin blood smears were prepared and stained with Giemsa (Guri®). Thick blood smears were used to enumerate parasitaemias below 1% by the Earle Perez method [59]. Once parasitaemia was greater than 1%, thin blood smears were used for parasitaemia measurements by determining the number of infected red blood cells (iRBCs) out of 1,000 total RBCs. The number of parasites per microlitre of blood was calculated from thin blood smears by multiplying the percentage of iRBCs by the number of RBCs per microlitre of blood obtained from the CBCs. Cumulative parasitaemia was calculated for each animal by adding together the daily parasitaemia (parasites/μl) from the day of inoculation to the day of necropsy. Mean parasitaemia across five-day increments was calculated for each individual by defining 5-day windows starting from the day of inoculation and averaging the parasitaemias within each window. Subsequent calculations with haemoglobin levels and platelet counts were likewise performed in this manner.

Quantification of parasite replication rate

The replication rate of parasites was calculated as described previously [60]. Only the first peak was considered because it had the most robust sample size.

Tissue collection, preservation, and pathology analysis

Tissues were collected at necropsy from 22 organs from all longitudinal infection experiments with the exception of E33, which had an abbreviated tissue collection, restricted to liver, lung, kidney, spleen, adrenal gland, BM, stomach, duodenum, jejunum, and colon where previous pathology had been observed. Gross lesions were photographed, and tissue sections were collected for histopathology. Each was preserved in 10% neutral buffered formalin, embedded in paraffin, sectioned at 4 mm, and stained with haematoxylin and eosin (H&E). Diagnostic characterization and scoring of histopathology were obtained from examination of randomized, blinded H&E-stained tissues. Tissues were scored from 1 (low) to 4 (high) based on: inflammation, oedema, necrosis, haemorrhage, hyperplasia, fibrosis, and vasculitis. The scores were summed and whole organ scores obtained for comparison, as described previously with *P. vivax*-infected *Saimiri boliviensis* tissues [61].

iRBC quantification within tissues

iRBC densities in the tissues were determined by counting the number of iRBCs in ten HPFs (1000×) under oil immersion on a standard light microscope, as described previously with *P. vivax* infected *S. boliviensis* tissues [61]. All sections were randomized and blinded.

Erythroid progenitor measurements by flow cytometry

Five µl of BM aspirate were placed into a 5 ml FACS tube. An antibody cocktail consisting of the antibodies outlined in Additional file 9: Table S9 was then added to each tube. The samples were vortexed and incubated at RT for 15 min in the dark. The samples were washed with 500 µl of PBS followed by centrifugation at 800×g for 7 min at 4 °C. The supernatant was aspirated and discarded. Hoechst 33342 dye (10 µg/ml) was then added to each sample and incubated for 30 min at 37 °C in the dark. Five hundred microlitres of PBS were then added to each sample followed by centrifugation at 800×g for 7 min at 4 °C. The supernatant was then aspirated and discarded. Samples were resuspended in 100 µl of 1X Annexin V binding buffer followed by addition of the Annexin V probe. After the samples were incubated for 15 min, an additional 400 µl of binding buffer was added, and the samples were immediately acquired on an LSR-II flow cytometer using standardized acquisition template.

Voltage was controlled throughout each longitudinal experiment by calibrating the instrument using rainbow calibration particles (Biolegend). After acquisition, data were compensated in FlowJo (Treestar, Inc), and then, uploaded to Cytobank for analysis. Frequencies of erythroid cells out of the erythroid population were exported and used in analyses. Other markers in the panel were either not significantly different or are beyond the scope of this manuscript.

Erythropoietin quantification

Erythropoietin (EPO) was measured as previously described [62] with minor modifications. Frozen plasma isolated from whole blood collected in EDTA was thawed on ice. Each aliquot was then centrifuged at 750×g for 15 min at 4 °C. The supernatant was collected and used in the Quantikine IVD ELISA kit from R&D systems following the manufacturer's suggested protocol except that the amount of suggested sample for the assays was reduced by 50% compared to what is suggested. EPO concentrations were determined using a 5-point standard curve that best fit the dynamic range of where the samples fell on the curve.

Computation of the removal of uninfected RBCs

The degree of removal of uninfected RBCs was computed with a discrete recursive mathematical model of the RBC dynamics, as previously performed for data generated from macaques infected with *P. cynomolgi* or *Plasmodium coatneyi* [63, 64]. Briefly, modelling the infection trajectory of each monkey was accomplished by fitting an adaptation of the former model [64, 65] to the experimentally determined data. The model has four variables, representing reticulocytes, RBCs, iRBCs and free merozoites. The first three have a lifetime age-structure stratified into 1-h intervals, while the iRBCs are modeled with only 24 one-hour age-classes, thus enforcing the approximate 24-h cycle of *P. knowlesi*. The model was parameterized with an RBC hazard function determined for rhesus macaques [64] using data from [66]. This hazard function allows the estimation of the level of RBC loss due to senescence. All other model estimates, reticulocyte maturation time, erythropoietic output, RBC loss due to the bystander effect, RBC loss due to parasitisation and immune responses against iRBCs, are determined in a "personalized" manner, namely based on experimental data generated from each animal. The full model description can be found elsewhere [64].

Statistical analyses

Data were generally divided into two categories for these analyses. Samples that were collected daily, namely

parasitaemias, haemoglobin, reticulocyte counts, and platelet counts were divided into 5-day intervals and compared across the course of infection using a linear mixed effects model that accounted for date and monkey drop out due to sacrifice (Additional file 10: Fig S1, Additional file 11: Fig. S3). Direct comparisons of tissue scores were performed using a Tukey HSD test. Statistics and figures were produced in R Studio version 1.1.383, under R version 3.4.3 GUI version 1.70, or JMP Pro version 13.0.0. Associations were tested using the Spearman's correlation test, and hierarchical multiple linear regression analyses. Multicollinearity was assessed using the *olsrr* package in R. Graphs were prepared using JMP Pro version 15. Comparisons were considered significant when FDR-adjusted, where appropriate, p-values below 0.05.

Results

Fifteen malaria-naïve *M. fascicularis* comprising three experimental cohorts (E07, E33, and E35), in addition to three control monkeys (E34), were assigned to this study and used sequentially in a set of iterative longitudinal *P. knowlesi* infection experiments. Brief accompanying details about the animal cohorts and experimental plans are summarized in Additional file 1: Table S1. Schematics showing the timeline from the time of the telemetry device implantation and activation to record data (for E07 animals) with the projected and actual parasitaemias, as well as sampling and necropsy time points for all of the animals by cohort are displayed in Additional file 10: Fig. S1, Additional file 11: Fig. S2, Additional file 12: Fig. S3.

Kra monkeys controlled acute *P. knowlesi* parasitaemia and developed chronic infections without anti-malarial intervention

All kra monkeys infected in this study ($n = 15$) developed patent blood-stage infections 6–7 days post-inoculation (dpi) with cryopreserved *P. knowlesi* sporozoites, and they controlled the acute phase parasitaemia within a few days without the need for anti-malarial intervention (Figs. 1a, 1b). The average *P. knowlesi* parasite replication rate between patency and peak parasitaemia was 8.59-fold \pm 1.719 (mean \pm SEM) per cycle, which is comparable to the value of tenfold, which is accepted in the literature and was determined for rhesus monkey infections with *P. knowlesi* and in vitro culture using rhesus erythrocytes [44, 45, 67]. Most primary parasitaemic peaks averaged about 1000 parasites/ μ l; however, three of the 15 monkeys developed parasitaemias that exceeded 40,000 parasites/ μ l, which is equivalent to about 1% iRBCs out of the total RBCs enumerated (Fig. 1a). To

identify the time where the kra monkeys began controlling the parasitaemia and when chronic infections began to develop, the mean parasitaemia across five-day increments was calculated for each individual and compared. Parasitaemias peaked 6–15 dpi, declined significantly by 21–25 dpi, and began to stabilize by 31–35 dpi where they persisted at or below 200 parasites/ μ l (Fig. 1c). Overall, the parasitaemia kinetics in the kra monkeys was similar to those reported in previous studies irrespective of the *P. knowlesi* infections being initiated with sporozoites or blood-stages [40, 44, 45, 52]

Kra monkeys infected with *P. knowlesi* developed mild to moderate thrombocytopenia

Platelet levels were stable in the *P. knowlesi*-infected kra monkeys through 7 dpi, and then they began to rapidly decrease through 10 dpi while parasitaemia was rising, even though this decrease was not significantly different (Fig. 2a). After parasitaemias peaked, platelet counts began increasing and returned to baseline levels by 21–25 dpi (Fig. 2a, b). The monkeys experienced mild to moderate thrombocytopenia, as reported previously for *P. cynomolgi* and *P. coatneyi* infection of rhesus monkeys [58, 66, 68], with platelet nadirs as low as 129,000 platelets/ml (Fig. 2a). Importantly, none of the animals developed severe thrombocytopenia, defined as platelet nadirs below 50,000 platelets/ μ l [69]. As platelet levels decreased, the mean platelet volume (MPV) remained high but then significantly declined after about 13 dpi and remained lower than baseline throughout the rest of the infection (Fig. 2c).

Moderate to severe anaemia developed during *P. knowlesi* infections in kra monkeys due to removal of uninfected RBCs and not inefficient erythropoiesis

Haemoglobin levels in the infected kra monkeys were determined daily by CBC analysis to evaluate the development of anaemia. Haemoglobin levels were stable through 8–10 dpi, but then sharply decreased after the peak of parasitaemia through 20 dpi (Fig. 3a, b). Two monkeys developed haemoglobin nadirs as low as 4.8 g/dL, corresponding to severe anaemia (< 7.0 g/dl) with about a 55% loss in haemoglobin relative to baseline (Fig. 3a, b). Haemoglobin levels began to increase about 21 dpi and continued to increase throughout the remainder of the infection period (Fig. 3a, b). Despite the dramatic loss in haemoglobin, the haemoglobin levels rebounded without anti-malarial or clinical intervention and were on average greater than 11 g/dl by 36 dpi until the end of the study (Fig. 3a, 3b). Mild anaemia persisted until the end of the experiment, and the animals never

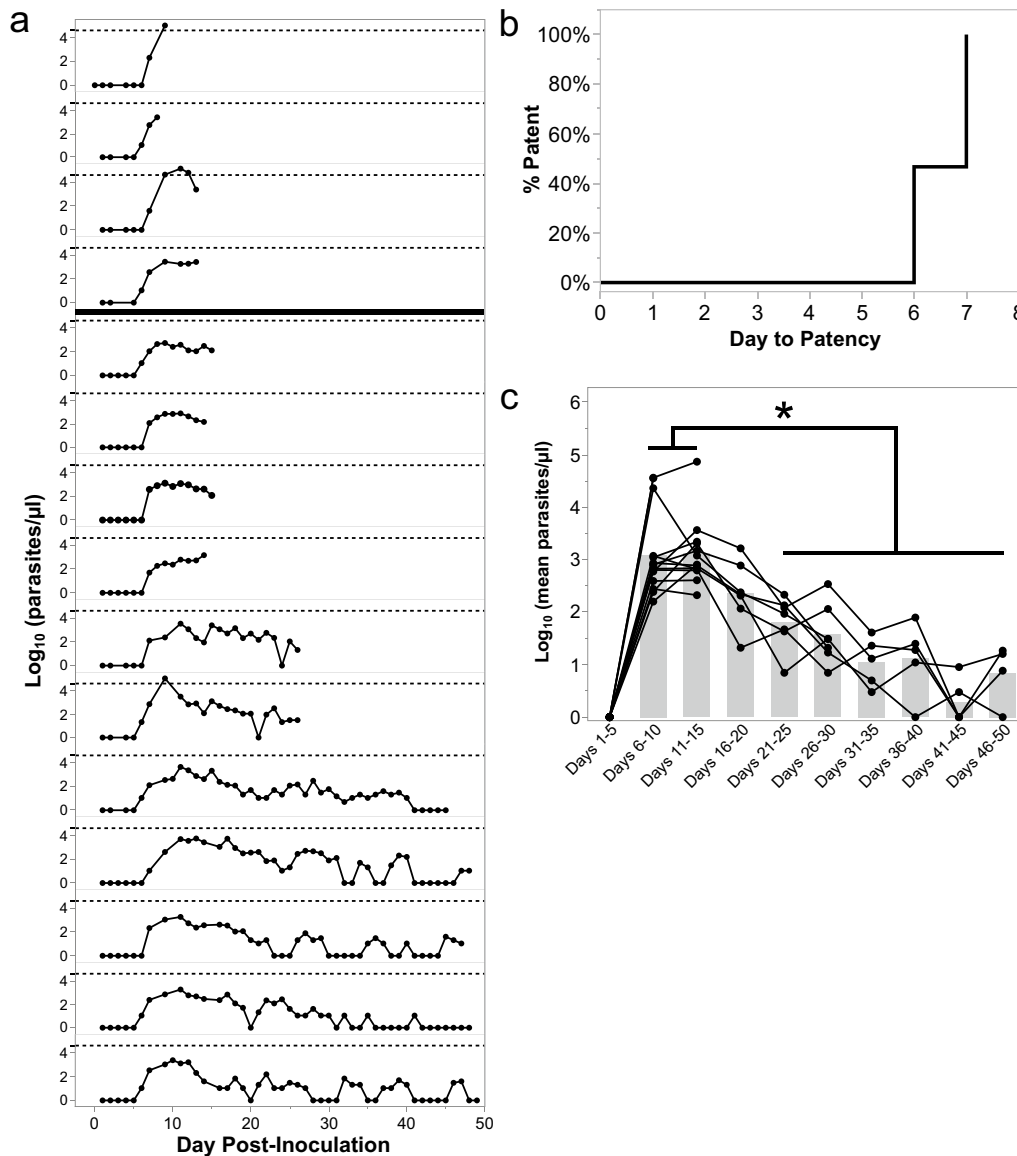
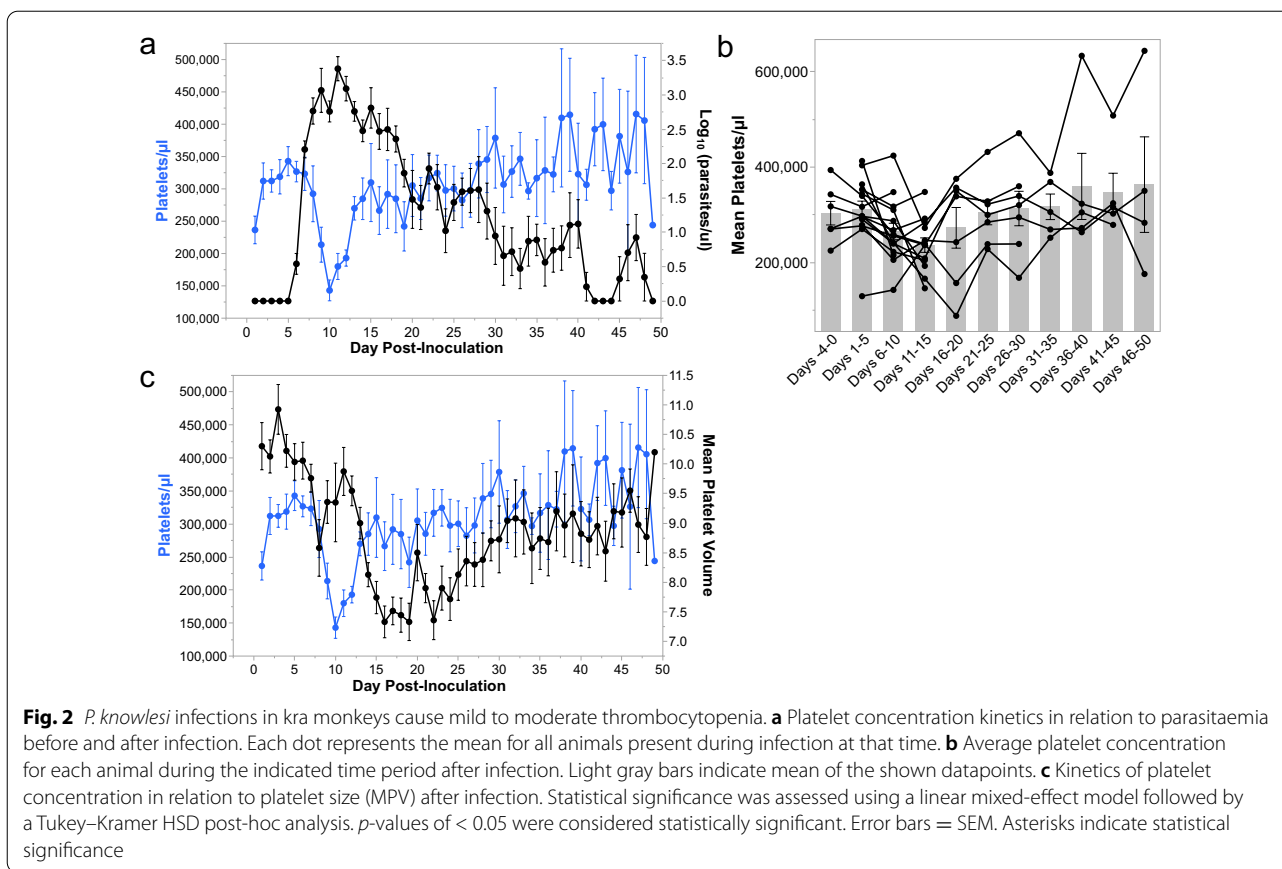


Fig. 1 *Plasmodium knowlesi*-infected kra monkeys control parasitaemia without antimalarial treatment and develop persisting parasitaemias. **a** Afternoon peripheral parasitaemias determined by thick and/or thin blood films for 15 kra monkeys infected with about 100,000 cryopreserved *P. knowlesi* H strain sporozoites. Dashed line indicates approximately 40,000 parasites/ μ l or about 1% parasitaemia. The four animals above the bold horizontal line were sacrificed during the acute phase, and the 11 below were sacrificed after parasitemia became chronic. **b** Time to patency analysis for the 15 kra monkeys shown in **a**. **c** Average parasitaemia for each animal during the indicated time period after infection. Light gray bars indicate mean of the shown datapoints. Statistical significance was assessed using a linear mixed-effect model followed by a Tukey–Kramer HSD post-hoc analysis. *p*-values of < 0.05 were considered statistically significant. Asterisks indicate statistical significance

fully recovered to their pre-infection haemoglobin levels (Fig. 3a, b), akin to previous reports with patients [24].

Inefficient erythropoiesis was shown to be a contributor in the development of malarial anaemia in rhesus monkeys with *P. coatneyi* or *P. cynomolgi* infections [62, 66], as well as in humans and rodents infected with malaria parasites [70–73]. Thus, it was hypothesized

that inefficient erythropoiesis may contribute, at least in part, to the development of anaemia in *P. knowlesi* infected kra monkeys. Contrary to this hypothesis, however, peripheral reticulocyte counts steadily increased as haemoglobin levels decreased, and they peaked a couple of days after the haemoglobin levels reached their nadirs (Fig. 3c–e). To evaluate if the increase in reticulocyte



levels was appropriate to compensate for the decrease in haemoglobin levels, the RPI was calculated. Indeed, the RPI was sustained over 2 from about 17–26 dpi, indicating that there was adequate compensation by the BM, following the dropping haemoglobin levels, and no evidence of inefficient erythropoiesis was found (Fig. 3e).

To confirm if the increase in peripheral reticulocyte levels was due to upregulation of erythropoiesis in the BM, the frequency of erythroid lineage cells in the whole BM aspirates collected prior to infection and at 8–11 dpi was evaluated by flow cytometry. The gating strategy used to quantify the frequency of erythroid progenitor cells in the BM aspirates is described in Additional file 13: Fig. S4. The erythroid lineage cells were defined as CD41a-CD45-LiveDead-CD71+ Hoechst+ cells. The frequency of erythroid lineage cells was increased in the BM aspirates, acquired by 10 or 11 dpi, compared to baseline (Fig. 3f, g). Consistent with the flow cytometry data, H&E-stained BM specimens acquired at necropsies as early as 10 dpi revealed substantial expansion of erythroid progenitors relative to uninfected controls (Fig. 3h). Correspondingly, plasma EPO levels were significantly elevated above baseline levels at these times for a subset of animals where plasma samples were available (Fig. 3i).

Since there was no evidence of inefficient erythropoiesis in the *P. knowlesi*-infected kra monkeys and the relatively low parasitaemia could not account for the observed decrease in haemoglobin levels, the degree of removal of uninfected RBCs was computed using a mathematical model devised for this purpose [64]. Modeling of the kra monkey data showed an appropriate timely compensatory erythropoietic response, with $68.6\% \pm 4.9\%$ (mean \pm SEM) attributable to the removal of uninfected bystander RBCs (Fig. 3j). The model estimated that the parasite was responsible for less than 0.4% of the total RBC losses (Additional file 14: Fig. S5).

Kra monkeys infected with *P. knowlesi* developed fevers that self-resolved

Densely sampled temperature data were analysed from the kra monkeys that had surgically implanted telemetry devices (*n* = 7, E07, Additional file 1: Table S1 and Additional file 10: Fig. S1) to study their temperature patterns including possible fever after infection (Fig. 4a). Fever was defined as any increase above an individual’s baseline range of temperatures, which represent each monkey’s daily circadian rhythm. All kra monkeys exhibited a fever by 7 dpi corresponding

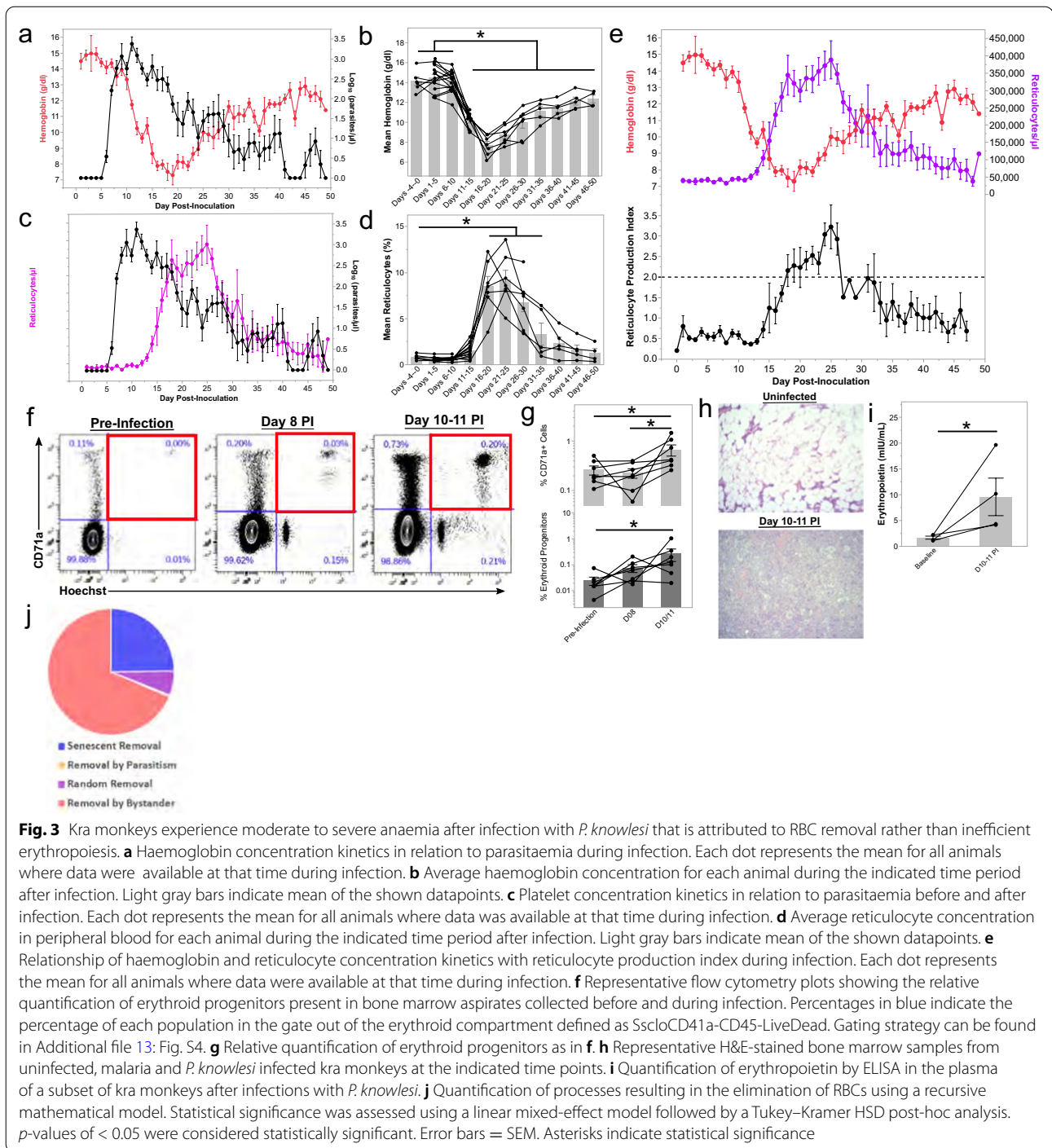


Fig. 3 Kra monkeys experience moderate to severe anaemia after infection with *P. knowlesi* that is attributed to RBC removal rather than inefficient erythropoiesis. **a** Haemoglobin concentration kinetics in relation to parasitaemia during infection. Each dot represents the mean for all animals where data were available at that time during infection. **b** Average haemoglobin concentration for each animal during the indicated time period after infection. Light gray bars indicate mean of the shown datapoints. **c** Platelet concentration kinetics in relation to parasitaemia before and after infection. Each dot represents the mean for all animals where data was available at that time during infection. **d** Average reticulocyte concentration in peripheral blood for each animal during the indicated time period after infection. Light gray bars indicate mean of the shown datapoints. **e** Relationship of haemoglobin and reticulocyte concentration kinetics with reticulocyte production index during infection. Each dot represents the mean for all animals where data were available at that time during infection. **f** Representative flow cytometry plots showing the relative quantification of erythroid progenitors present in bone marrow aspirates collected before and during infection. Percentages in blue indicate the percentage of each population in the gate out of the erythroid compartment defined as SsclCD41a-CD45-LiveDead. Gating strategy can be found in Additional file 13: Fig. S4. **g** Relative quantification of erythroid progenitors as in **f**. **h** Representative H&E-stained bone marrow samples from uninfected, malaria and *P. knowlesi* infected kra monkeys at the indicated time points. **i** Quantification of erythropoietin by ELISA in the plasma of a subset of kra monkeys after infections with *P. knowlesi*. **j** Quantification of processes resulting in the elimination of RBCs using a recursive mathematical model. Statistical significance was assessed using a linear mixed-effect model followed by a Tukey–Kramer HSD post-hoc analysis. *p*-values of < 0.05 were considered statistically significant. Error bars = SEM. Asterisks indicate statistical significance

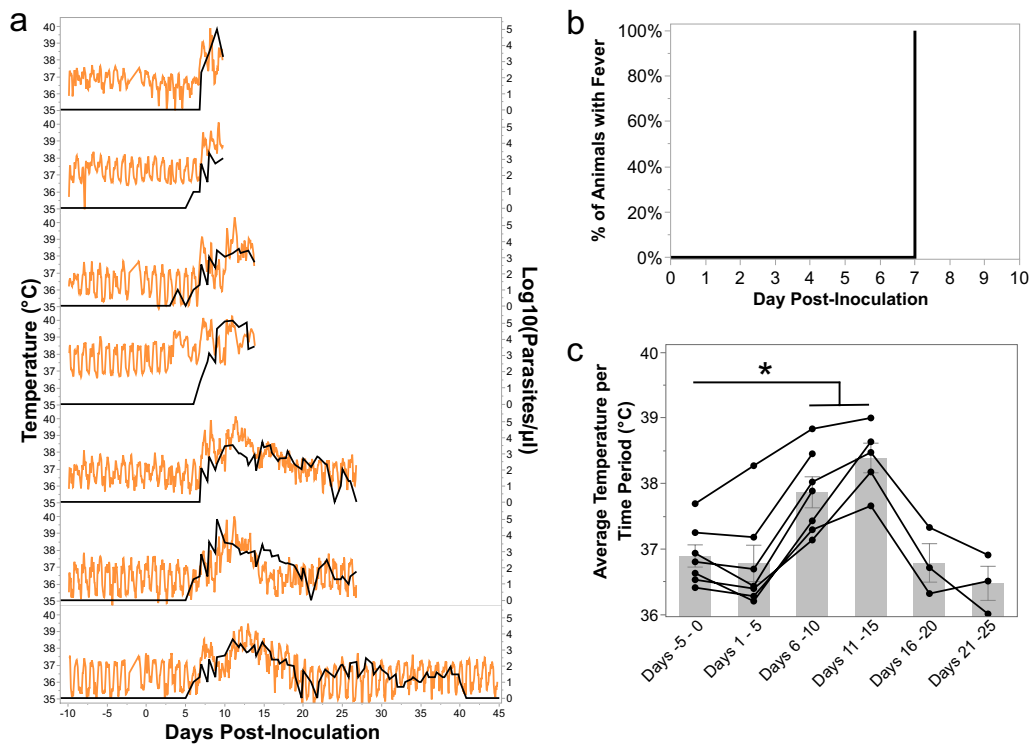


Fig. 4 Kra monkeys develop fevers shortly after patency, which resolve after the control of parasitaemia. **a** Temperature kinetics in relation to parasitaemia in animals that had telemetry devices surgically implanted. **b** Time to fever analysis using the telemetry data in **a**. **c** Average temperature for each animal during the indicated time period after infection. Light gray bars indicate mean of the shown datapoints. Error bars = SEM. Bar graphs and error bars represent mean \pm SEM. Statistical significance was assessed using a linear mixed-effect model followed by a Tukey–Kramer HSD post-hoc analysis. p -values of < 0.05 were considered statistically significant. Asterisks indicate statistical significance

roughly to the period in which the blood-stage infection reached patency, between 6 and 8 dpi (Fig. 4a, b). The average temperature of the animals significantly increased from pre-infection values of 36.89 ± 0.17 °C (mean \pm SEM) to 37.87 ± 0.24 °C and 38.39 ± 0.23 °C by 6–10 and 11–15 dpi, respectively (Fig. 4c). The febrile threshold [67] was defined as the parasitaemia at which the kra monkeys developed temperatures and determined to be about 160 ± 71.58 parasites/ml (mean \pm SEM). After parasitaemia was controlled, the average temperatures decreased to pre-infection

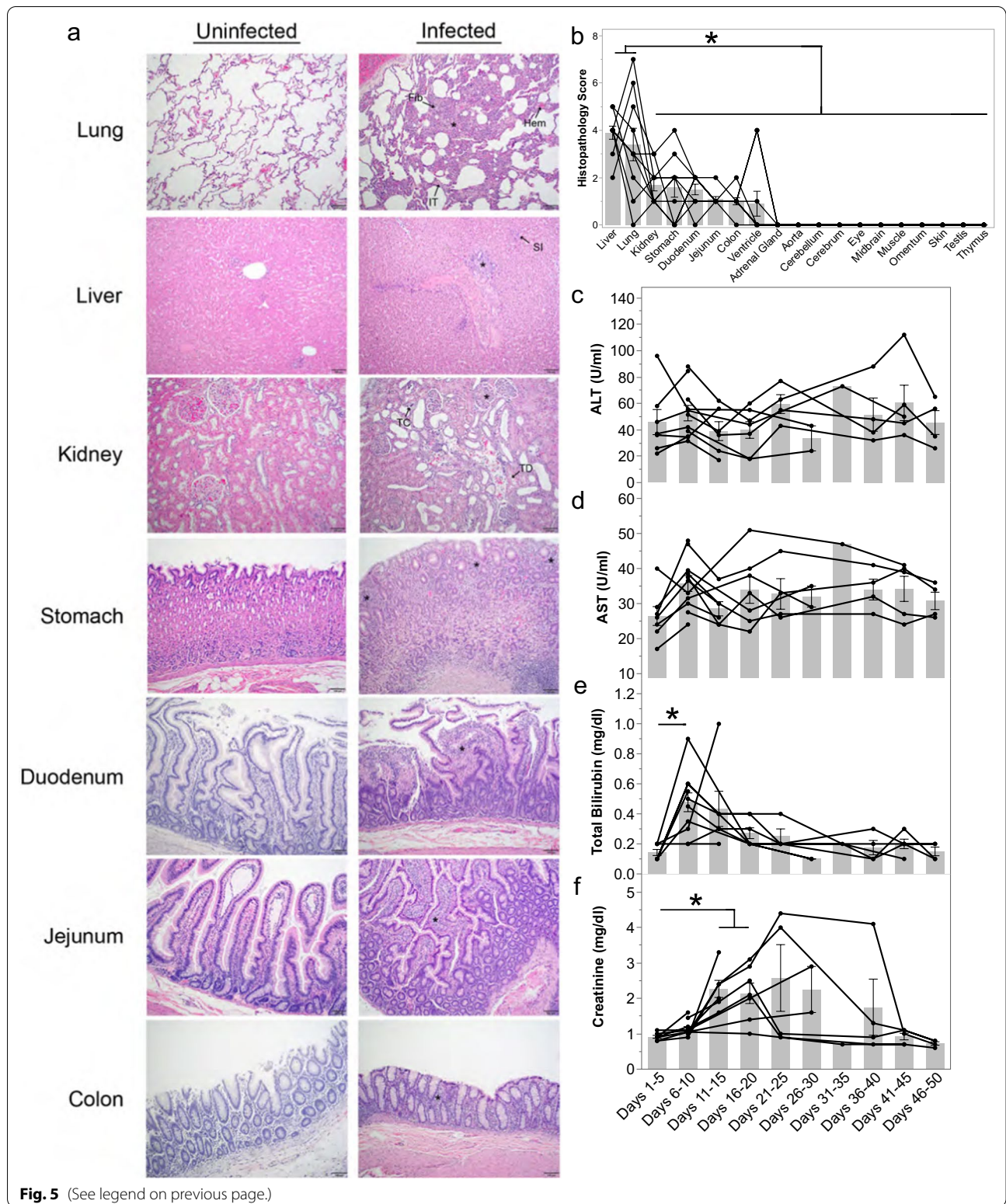
levels of 36.79 ± 0.29 °C and 36.48 ± 0.26 °C for the day 16–20 and 21–25 time periods, respectively (Fig. 4a and c). Monkeys that proceeded to establish chronic low-level parasitaemia no longer experienced temperature spikes (Fig. 4a, c).

***Plasmodium knowlesi* infection in kra monkeys caused mild to moderate tissue pathology**

An extensive analysis was performed of H&E-stained tissue sections acquired from up to 22 different organs collected from the *P. knowlesi*-infected kra monkeys,

(See figure on next page.)

Fig. 5 *Plasmodium knowlesi*-infected kra monkeys exhibit histopathology consistent with systemic measures of disease. **a** Representative light micrographs of H&E-stained tissue sections from control and infected kra monkeys. Infected lungs showed areas of fibrosis (Fib), hyperplasia (*), haemolysis (Hem), and interstitial thickening (IT). All animals had periportal (*) and sinusoidal (SI) infiltration in the liver. Kidney histopathology included tubular crystal formation (TC), hypercellular glomeruli (*), and tubular degeneration (TD). The stomach, duodenum, jejunum, and colon all exhibited mucosal immune infiltration (*). **b** Semi-quantitative histopathology scores of tissues collected at necropsy. The average alanine transaminase (**c**), aspartate aminotransferase (**d**), total bilirubin (**e**), and creatinine (**f**) for each animal where data were available during the indicated time period after infection. Light gray bars indicate mean of the shown datapoints. Error bars = SEM. Statistical significance was assessed using a linear mixed-effect model followed by a Tukey–Kramer HSD post-hoc analysis. p -values of < 0.05 were considered statistically significant. Asterisks indicate statistical significance



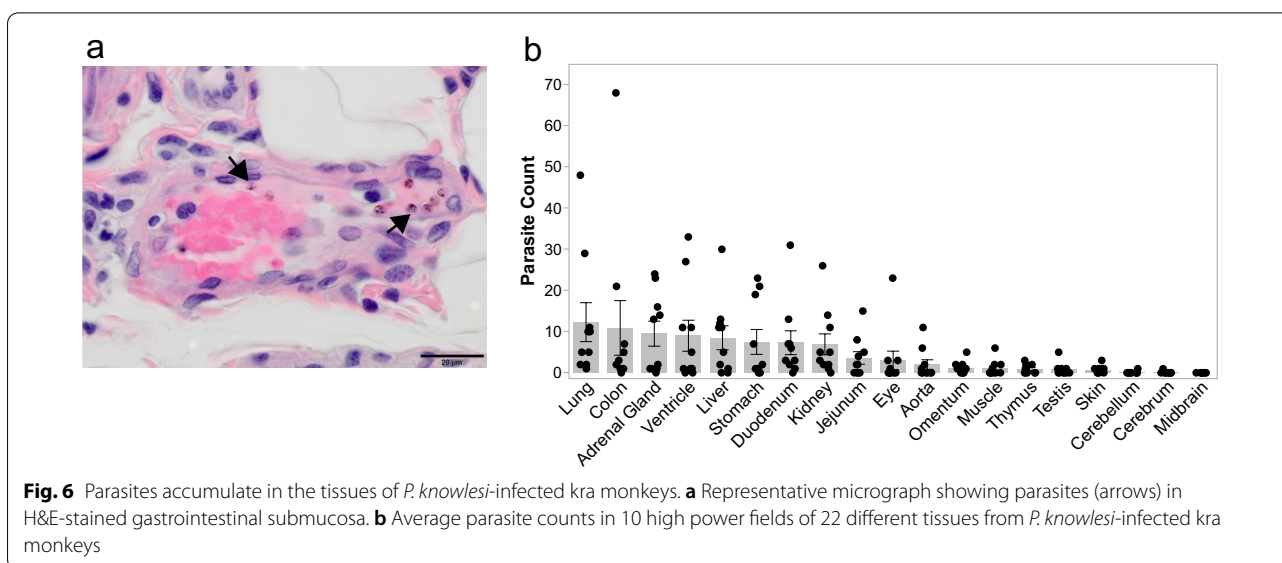
sacrificed at different dpi, to determine if and the extent to which the monkeys may have sustained tissue damage. Hyperplasia, interstitial thickening, and fibrosis were observed in the lungs of nearly all monkeys (13/15), and mild to moderate haemorrhage occurred in four of them (Fig. 5a and Additional file 2: Table S2). All monkeys had Kupffer cell hyperplasia and evidence of liver inflammation based on cellular infiltrates around the periportal region and congestion in the hepatic sinuses (Fig. 5a). No hepatocellular necrosis or cholestasis was noted. The kidneys of all animals showed glomerular hypercellularity without glomerulonephritis, and three animals had tubular degeneration (Fig. 5a and Additional file 2: Table S2). One monkey with high parasitaemia and elevated creatinine had evidence of calcification or crystalline deposition in the kidney tubules (Fig. 5a and Additional file 2: Table S2). Less common kidney pathologies included interstitial inflammation and haemorrhage (Additional file 2: Table S2). Gastrointestinal inflammation was observed in the tissues from each monkey and included gastritis, duodenitis, jejunitis, and mild colitis without oedema. The spleens from the infected animals were grossly enlarged and weighed significantly more than the spleens from uninfected animals; the day of necropsy did not influence these results (Additional file 3: Table S3). The adrenal glands, aorta, cerebrum, cerebellum, mid-brain, eyes, lymph nodes, omentum, skeletal muscle, testis, and thymus were unremarkable.

The severity of the observed tissue damage in each tissue except for the BM and spleen was scored for each animal to facilitate a semi-quantitative comparison of tissue damage between organs (Additional file 2: Table S2) as performed previously with tissues from *P. vivax*-infected

S. boliviensis monkeys [61]. The severity of tissue damage in the lungs and liver was significantly higher than other tissues that sustained pathology (Fig. 5b and Additional file 4: Table S4). The date of necropsy—which differed for the animals—did not affect the histopathological scores, indicating that how long an animal was parasitaemic did not have a detectable impact on the severity of tissue damage (Additional file 5: Table S5). In line with the absence of cholestasis and hepatocellular necrosis, aspartate aminotransaminase (AST) and alanine aminotransferase (ALT) remained unchanged during infection, and while bilirubinaemia was observed, it resolved by 11–15 dpi (Fig. 5e). Consistent with kidney pathology, serum creatinine levels were significantly elevated 11–20 dpi before returning to baseline levels (Fig. 5f). Notably, creatinine levels varied significantly between individuals after 20 dpi (Fig. 5f).

Parasite accumulation in the vasculature is associated with severity of tissue damage

To determine if the severity of damage in each tissue was associated with parasite accumulation within that tissue, the number of iRBCs in 10 high-power fields (HPFs) was enumerated (Additional file 6: Table S6). This analysis provided approximate iRBC densities within each tissue, for 22 tissue types, as also performed previously with *P. vivax*-infected *S. boliviensis* tissues [61]. A representative image of parasites identified in tissues is shown in Fig. 6a. Multiple analyses were then used to assess if the accumulation of parasites in the tissues was associated with the tissue damage scores (Additional file 2: Table S2). First, a univariate analysis was performed between tissue scores and iRBC density. Parasite iRBC burden



weakly positively correlated with tissue score ($\rho = 0.265$, p -value = 0.00022). Next, a hierarchical multiple linear regression analysis was performed to determine which factors affected tissue scores the most (Additional file 7: Table S7). A model considering only iRBC tissue burden did not result in a linear relationship (adjusted $R^2 = 0.0354$, p -value = 0.0054). However, when combined with the tissue type, the relationship was moderately linear (adjusted $R^2 = 0.678$, p -value = 2.2×10^{-16}), indicating that the iRBC burden in a tissue may contribute to the degree of damage observed. The day of necropsy, parasitaemia at necropsy, and cumulative parasitaemia were also tested and were found not to contribute to the relationship (Additional file 8: Table S8). No multicollinearity was noted.

Discussion

This longitudinal infection study defines clinical, physiological and pathological changes that occurred in kra monkeys after being experimentally infected with *P. knowlesi* sporozoites. Consistent with kra monkeys being a resilient host, they controlled their parasitaemia soon—within a few days—after becoming patent and did not develop severe thrombocytopenia, a complication that has been observed with severe human *Plasmodium* infections [reviewed in 69], and most notably with *P. knowlesi* [1, 24, 30], as well as some *P. cynomolgi* or *P. coatneyi* infections in rhesus monkeys [58, 66]. Recently, thrombocytopenia has been associated with platelet-*Plasmodium* iRBC interactions that result in the killing of those infected cells [74]. While platelet killing of *P. knowlesi*-iRBCs was not evaluated in the current study, it is certainly conceivable that platelets could have a killing function in this animal model. In fact, the mild thrombocytopenia observed here would be fitting with platelets having a role in eliminating parasites and contributing to the lower level of iRBCs in this resilient host. It would be of extreme interest to test this possibility and establish direct comparisons of parasitaemia and thrombocytopenia with platelet killing assays also performed during rhesus infections, where the parasitaemia escalates unabated to high levels.

A precipitous and dramatic drop of haemoglobin occurred during the peak of *P. knowlesi* parasitaemia in the kra monkeys and continued until the parasitaemia was controlled. This resulted in haemoglobin nadirs within the documented range of moderate to severe malarial anaemia experienced by *P. cynomolgi* or *P. coatneyi*-infected rhesus macaques [58, 66, 68, 75], humans with *Plasmodium* parasites [reviewed in 76], and notably children with *P. knowlesi* [31]. These haemoglobin kinetics are reproducible in NHPs infected with *Plasmodium* spp. and virtually indistinguishable from the

haemoglobin kinetic data generated retrospectively from neurosyphilitic patients infected with *P. vivax* [77]. The development of severe anaemia in kra monkeys infected with *P. knowlesi* has not been previously reported and these data raise the intriguing point that these animals demonstrated natural resilience to their infection despite demonstrating this disease manifestation. This raises questions regarding what mechanisms are used by these animals to overcome the anaemia.

Interestingly, in this regard, in contrast to inefficient erythropoiesis reported for humans, rhesus macaques, and rodents infected with malaria parasites [62, 66, 68, 70–73, 75], there was no evidence in the *P. knowlesi*-infected kra monkeys that inefficient erythropoiesis contributed to the development of their anaemia. Instead, the kra monkey BM responded appropriately when EPO was elevated in the plasma, comparable to data shown recently for four kra monkeys infected with *P. coatneyi*-infected RBCs and monitored for anaemia [75]. Thus, the mechanism(s) that apparently limits an EPO-dependent response to malarial anaemia in humans, rhesus macaques, and rodent malaria parasite model systems, appears to be absent in kra monkeys, thereby, enabling kra monkeys to sufficiently compensate for the loss of RBCs during *P. knowlesi* malaria. The data presented here suggest that preserving the BM's ability to compensate for the loss of RBCs is a noteworthy characteristic of resilience displayed by the kra monkeys to *P. knowlesi* infections. Future comparative studies should explore soluble factors, such as inflammatory molecules, metabolites, growth factors, that are different between kra and rhesus monkeys infected with *P. knowlesi* to identify factors that may contribute to inefficient erythropoiesis in the rhesus but not the kra monkey.

Previous malarial anaemia studies based upon rhesus macaques infected with *P. cynomolgi* or *P. coatneyi* could not readily distinguish the contribution of inefficient erythropoiesis versus removal of uninfected erythrocytes because these processes occurred sequentially [58, 66, 68, 75]. In rhesus macaques infected with *P. cynomolgi* or *P. coatneyi*, there is apparent inefficient erythropoiesis that occurs while haemoglobin levels begin to drop [58, 66, 68, 75]. This is followed by a rapid decline in haemoglobin levels despite a compensatory response by the BM [58, 62, 66, 68, 75]. Mathematical modelling of RBC haemodynamics in rhesus monkeys infected with *P. coatneyi* suggested that removal of uninfected erythrocytes contributed more to anaemia in the *P. coatneyi* infected rhesus monkeys than inefficient erythropoiesis [63]. Significant loss of uninfected RBCs was also predicted based on the retrospective modelling of *P. falciparum* parasitaemia and anaemia data from neurosyphilis patients undergoing malariotherapy [78] and

demonstrated in clinical studies involving *P. falciparum* and *P. vivax* [79]. Still, the extent that inefficient erythropoiesis contributed to the exacerbation of anaemia in the animal models, dominated by the removal of uninfected RBCs, remained unclear. Curiously, the kra monkeys in this study displayed no evidence of inefficient erythropoiesis yet maintained similar adverse haemoglobin kinetics as determined from rhesus monkey models [58, 62, 66, 68, 75] and human data [reviewed in 76]. In kra monkeys infected with *P. coatneyi*, the observed erythropoietic response was suboptimal, and alone did not explain the anaemia observed in this species [75]. Overall, with malaria caused by various *Plasmodium* species, it appears that the removal of uninfected RBCs may contribute more than inefficient erythropoiesis to the development of malarial anaemia than previously appreciated, as also generally concluded by Jakeman et al. [78].

The mathematical model suggests that only 0.4% of RBC losses in kra monkeys are directly due to infection by *P. knowlesi*, while 31% are removed by normal physiologic processes of cellular senescence and random death, which do not contribute to the anaemia. That leaves 68.6% of losses unaccounted, and hence attributed to the bystander effect. A possible alternative explanation could be that large numbers of iRBCs might be hiding in peripheral tissues, thereby making the circulating level of iRBCs appear low, while still contributing to the overall production of parasites. This explanation does not seem probable though, as rather few iRBCs were identified in peripheral tissues, where the levels correlated with the small numbers observed in circulation. Furthermore, in order to exclude the high degree of bystander removal, the total number of iRBCs would have to be two orders of magnitude higher, which seems very unlikely. Thus, as these monkeys showed a normal compensatory BM response, the most likely explanation appears to be that a process of substantial bystander destruction of RBCs is induced in order to remove as many of the iRBCs as possible while also reducing the pool of infectable RBCs. Both processes would result in a slower growth of the parasite population, which would afford the host valuable time to launch an adaptive immune response. This process might involve platelets, which would explain the often-observed malarial thrombocytopenia [69].

Kra monkeys infected with *P. knowlesi* are well-suited to study the possible physiological and immunobiological mechanisms that lead to the removal of uninfected RBCs, whether in malaria-naïve or semi-immune animals [66]. Interestingly, recent RBC deformability studies showed that the ability of uninfected RBCs to become deformable was not affected in *M. fascicularis* ($n = 3$, bred and grown in animal facilities at Nafovanny in a malaria-free environment in Vietnam) after being infected for 8 days

with *P. knowlesi* (UM01 strain) blood-stage parasites, and echinocyte formation was not observed [54]. These findings contrast with that group's complementary results from human infections [54], and published findings from infected rhesus monkeys (*Macaca mulatta*) [80, 81], in support of the idea that the absence of these adverse rheologic features and the maintained deformability of RBCs in the kra monkeys supports their resilience. Future studies are warranted that look more closely at all of these factors side-by-side with both monkey species, to hone in on the various mechanisms that may support the resilient phenotype.

Acute *Plasmodium* infections caused by different parasite species—whether in NHPs or humans—are known to cause damage to tissues and vital organs and contribute to clinical complications and possibly death [reviewed in 37]. Anderios et al. described histological changes in the spleen and liver of two kra monkeys (born and bred at the Institute for Medical Research in Kuala Lumpur) after 60 or 90 days of infection with blood-stage parasites derived from the blood of a human patient or a cryopreserved isolate from an infected rhesus (obtained from the American Type Culture Collection (ATCC)) [53]. The current longitudinal study with 15 kra monkeys is much more comprehensive with the histopathological analysis of 22 tissues. Here, histological changes in the liver, lungs, kidneys, and the gastrointestinal tract were identified, but consistent with kra monkeys being a resilient host, the tissue lesions observed were relatively mild, and this was so regardless of whether the tissues being analysed were from acutely or chronically infected animals (Additional file 2: Table S2). These results can be contrasted with the severe tissue damage previously reported from *P. knowlesi*, *P. coatneyi* or *P. cynomolgi* infections in rhesus macaques [50, 82–85].

Consistent with the mild histological changes observed in this study of kra monkeys, there were only a few indications of organ dysfunction. Nearly all animals had some degree of tissue damage in the lungs, and the lungs had the highest iRBC count per high power field. Creatinine levels became elevated at the peak of parasitaemia and remained elevated, indicative of kidney issues. Given the minor tissue-damage observed in the kidneys, it is possible that the increased creatinine could be related to an increase in antigen–antibody immune complex deposition in the kidney tubules or a decrease in fluid intake. Regardless, it is relevant to note that increased creatinine has been a common finding in patients with severe malaria [34]. Hyperbilirubinaemia has also been associated with severe *P. knowlesi* malaria in humans [24]. Likewise, bilirubin was elevated in the kra monkeys. Although direct and indirect bilirubin levels were unavailable, the absence of significant histological evidence for hepatic

injury such as cholestasis suggests that the elevated total bilirubin levels in the kra monkeys were due to hemolysis of uninfected RBCs. In agreement with this hypothesis, bilirubinaemia returned to baseline in the latter part of the infections, coincident with the recovery of haemoglobin levels. Neither ALT nor AST were elevated at any stage in the infections, which is consistent with the absence of hepatocyte necrosis, or signs of major tissue damage systemically. Together, these data suggest that kra monkey resilience to *P. knowlesi* infection, as demonstrated by their control of parasitaemia and compensation for anaemia, is reflected by only minimal or mild tissue damage and organ dysfunction.

The presence of iRBCs in various tissues have been reported from previous studies with *P. knowlesi* infected rhesus macaques [49, 50]. Likewise, *P. knowlesi* iRBCs were identified in the tissues of the kra monkeys in this study and they predominated in the spleen, adrenal glands, lungs, kidneys, and gastrointestinal tract. However, relatively few iRBCs were identified, which is consistent with the comparatively low number of circulating parasites in the resilient kra monkey species. Regardless, similar as determined in prior studies with *P. vivax* infection of *S. boliviensis* monkeys [61], there was a modest relationship in the current study between histopathology score and parasite accumulation in the tissues.

Understanding the immune responses and pathophysiological processes that occur during *P. knowlesi* infections in humans has been of great interest but studying these infections longitudinally in humans is not feasible due to ethical requirements to treat individuals once they are parasitaemic. *Plasmodium knowlesi*-infected kra monkeys are a viable alternative for studying the progression of acute and chronic infections, and without drug treatment being a confounding factor. Unlike infections of rhesus monkeys with various *Plasmodium* species, the *P. knowlesi*-infected kra monkeys uniformly develop naturally occurring chronic infections [44, 45, 51, 52], and with similarly low parasitaemia levels as recorded for uncomplicated *P. knowlesi* infections in humans [24]. Importantly, while the kra monkeys demonstrated resilience from severe and deadly disease, chronicity was characterized similar to human infections by persistent and lower than normal haemoglobin levels. These results warrant further exploration in the context of this animal model to understand the loss of the uninfected RBCs and to determine what host responses may be occurring.

Interestingly, *P. knowlesi* infections in humans induce fevers at lower parasitaemias than *P. falciparum* infections [30]. Given recent findings that macaque RBC culture-adapted *P. knowlesi* parasites could be adapted to human RBCs by acquisition of sialic acid-independent invasion mechanisms, one hypothesis to explain this is

that *P. knowlesi* is not as well-adapted to humans, and, thus, can trigger immune responses more quickly than *P. falciparum* [86]. Therefore, it was expected that kra monkeys, as a natural host of *P. knowlesi*, would develop fevers once high parasitaemias developed. However, the kra monkeys developed fevers shortly after their infections reached patency, and their pyrogenic thresholds were about 160 parasites/ μ l. These data suggest that the lower pyrogenic threshold observed for *P. knowlesi* in humans may not solely be due to poor adaptation to humans. Kra monkeys may have evolved adaptations in pattern recognition receptors that enable them to detect parasite-derived molecules at lower levels than other primates, thereby, enabling the immune system to detect and respond to *P. knowlesi* more quickly, as shown in one study with a few animals [51].

As this research field advances, delving deeper into specific host-parasite interactions and pathways, it is important to take into consideration the origin and genetic background of the host monkeys and the infecting parasites, as well as prior experimental history of the animals and whether experiments are initiated with sporozoites or blood-stage parasites. The source and validation of the monkey and parasite species are critical. Thus, we have taken care to indicate the macaque monkey and *P. knowlesi* parasite sources and isolate information in this manuscript, and to the extent available for referenced papers [53, 54]. As early as 1932, major differences and nuances of *P. knowlesi* parasite-host combinations were described by Napier and Campbell [87] and Knowles and Das Gupta [43], and such data summarized then from numerous NHP infections, and since by others [44, 45, 88, 89], including instances of “hybrid” short-tailed kra/cynomolgus-rhesus monkeys [88], may bring important if not critical insights and value to current research.

Conclusions

This study reports a systematic analysis of *P. knowlesi*-infected kra monkeys to identify basic features of resilience to malaria, which could be relevant for infections caused by various species of *Plasmodium*. This investigation affirms previous reports that kra monkeys are resilient to *P. knowlesi* infections and shows that their resilience is not—at least in part—because they completely subvert development of clinical signs of malaria and avoid tissue-damage. Instead, while kra monkeys prevent *P. knowlesi* parasitaemia from rising above 1–3% they mount compensatory physiological responses that may reverse disease progression and limit tissue pathology. The kra monkey-*Plasmodium* infection model system is valuable for studying mechanisms of resilience to malaria and identifying specific physiological and immunobiological responses that may function to minimize

disease and death in people infected with *Plasmodium*. Of note, the kra monkey data best reflected the clinical picture of children rather than adults infected with *P. knowlesi*, as determined in a few studies [31–33]. Continued validation of this animal model is warranted as a complement to human studies aimed at understanding mechanisms of resilience to malaria, with the possible goal of new host-directed therapies to resolve acute disease states and the progression of chronic *Plasmodium* infections. Such inquiry has begun, specifically, for example, involving in-depth analysis of the peripheral blood transcriptomes of rhesus and kra monkeys in response to *P. knowlesi* [90].

Supplementary Information

The online version contains supplementary material available at <https://doi.org/10.1186/s12936-021-03925-6>.

Additional file 1: Table S1. Macaque Cohort and Experimental Summaries. Details regarding four monkey cohorts involved in the current study are summarised; three of these were experimentally infected with *P. knowlesi* sporozoites, and one served as control group. The cohorts are listed in the order in which experiments using these animals were performed. These animals and their longitudinal infection designs were part of a systems biology program, with iterative cohort experimentation designed to satisfy the goals of those research programs. [§]The non-sequential experimental numbering (E07, E33, E34, and E35) reflects the experimental numbers assigned in the MaHPIC Laboratory Information Management System. [†]Telemetry data were collected in E07 (only), for temperature, blood pressure, heart rate and activity level (Brady et al., manuscript in preparation). Spx is an abbreviation for splenectomy.

Additional file 2: Table S2. Histopathology scores for *P. knowlesi*-infected kra monkeys. The kra monkey codes shaded with PINK (n = 4) represent animals sacrificed during an acute phase of the infection, and the codes shaded with GREY (n = 12) represent animals sacrificed during a chronic phase of infection. The experimental number for each coded animal is also shown: E07, E33, or E35. Nineteen tissues were examined by a veterinary pathologist and scored semi-quantitatively in the categories above. Spleen, lymph nodes, and bone marrow were not scored because the changes were deemed to be physiological reactions to infection and/or anaemia. The following tissues were examined for histopathological changes, but omitted from this table because no changes were found: aorta, adrenal gland, cerebellum, eye, midbrain, muscle, skin, testis, thymus, and omentum. These tissues were assigned a score of zero for modeling purposes. Semi-quantitative scores are presented as a heatmap to visually represent severity, with 0 being no changes or damage, and 4 being diffuse changes. Organs were scored in several categories, including inflammation, oedema, crypt inflammation (for the gastrointestinal organs), necrosis, haemorrhage, hyperplasia (including alveolar wall thickening/interstitial hyperplasia, for the lungs, Kupffer cell hyperplasia in the liver, and glomerular hyperplasia for the kidneys), fibrosis, vasculitis, and tubular degeneration (for kidneys). The histopathology categories shown reflect the range of pathologies noted, whether for one or multiple monkeys.

Additional file 3: Table S3. Linear regression: spleen weight vs. time of infection. The effect of time at necropsy on spleen weight was tested via a linear regression model and found not to contribute.

Additional file 4: Table S4. Tukey HSD Post-hoc pairwise comparison of tissue score. Semiquantitative tissue scores were compared pairwise using Tukey HSD post-hoc analysis. Mean difference is the difference in means between the organ pair being compared. Adjusted *p*-value, significance

and upper and lower bound are included. **p* < 0.05; ***p* < 0.005, ****p* < 0.0005, *****p* < 0.00005; NS = not significant.

Additional file 5: Table S5. Linear regression: pathology score vs. necropsy day. The effect of time at necropsy on pathology score was tested via a linear regression model and found not to contribute.

Additional file 6: Table S6. Summary statistics for parasite tissue counts. Parasites in H&E-stained tissue sections for each organ were quantified by light microscopy. Mean number of parasites in 10 high power fields per H&E-stained tissue, standard deviation, standard error, and number of sections are presented.

Additional file 7: Table S7. Hierarchical Linear Regression Analysis. Multiple Linear Regression (MLR) was performed to test the relationship between score, count, and organ. For organ, adrenal gland was selected as the reference tissue. Parameter is significant at *p* = 0.05; **p* < 0.05, ***p* < 0.005, ****p* < 0.0005; NS = not significant.

Additional file 8: Table S8. Hierarchical Linear Regression Analysis of Infection Parameters. Multiple Linear Regression (MLR) was performed to test the relationship between score, count, days post-inoculation (DPI), parasitaemia, and cumulative parasitaemia. Parameter is significant at *p* = 0.05; **p* < 0.05, ***p* < 0.005, ****p* < 0.0005; NS = not significant.

Additional file 9: Table S9. Flow cytometry staining cocktail for measuring erythroid progenitors in rhesus and kra monkey bone marrow aspirates.

Additional file 10: Fig. S1. E07 Experimental Design and Parasitaemia, as also similarly presented in PlasmoDB [91] to accompany E07 publicly available data. Pilot *P. knowlesi* infection in seven kra monkeys (11C131, 11C166, 12C36, 12C44, 12C53, H12C59, H12C8) with staggered necropsy end-points that included necropsies at an acute (n = 4: 11C131, 12C36, H12C8, H12C59) or chronic (n = 3: 11C166, 12C44, 12C53) stage of infection. Top Panel: Schematic of the planned (generalized) experimental design with pre-infection surgical implantation of a telemetry device (scissors) plus recovery time and their activation for collection of physiological data, before (grey bar) and after surgery baseline timepoint (TP) sample collections (gold bars), *P. knowlesi* cryopreserved sporozoite inoculations at day 0 (syringe), predicted parasitaemia kinetics (pink curved line) with early infection, log-phase, peaking parasitaemia, and sequential chronic phase TPs indicated for blood and bone marrow sample collections. Necropsy endpoints (*) were planned for selected animals at an acute and early or late chronic stages of infection. Bottom Panel: Schematic showing E07 experimental data including *P. knowlesi* cryopreserved sporozoite inoculations on day 0 (syringe[†]), daily parasitaemias graphed (pink line), and defined TPs (gold bars) and the specific days of euthanasia and necropsy endpoints (*) are indicated for each of the animals. No subcurative treatments were required, as the blood-stage infections and clinical signs naturally began to resolve, as expected with kra monkeys. [†]This cohort had previously been inoculated with sporozoites freshly isolated from mosquito salivary glands, yet for reasons unknown, blood-stage parasitaemia did not result. Transcriptomic analysis of peripheral blood samples did not reveal any significant differences between these baseline TPs [55]. This pilot experiment allowed for (1) testing of cryopreserved stocks of *P. knowlesi* sporozoites and the kinetics of the parasitaemia in kra monkeys (pink line); (2) capturing blood, bone marrow and tissue data on both the acute and chronic phases of the infection; (3) testing of experimental and analysis pipelines for the generation and analysis of biological data at specific TPs, including the secure and reliable transfer of samples or data as required across the large MaHPIC and HAMMER consortia [92]; and collection and analysis of infected tissue samples from necropsies.

Additional file 11: Fig. S2. E33 Experimental Design and Parasitaemia, as also similarly presented in PlasmoDB [91] to accompany E33 publicly available data. E33 includes iterative *P. knowlesi* infections in a cohort of four kra monkeys (13C90, 14C15, 14C3, H13C110) to continue to study acute and early stage “Chronic I” infections. Top Panel: Schematic of the planned (generalized) experimental design with timepoints (TP) of sample collection (gold bars), *P. knowlesi* cryopreserved sporozoite inoculations at day 0 (syringe), predicted parasitaemia kinetics (pink line) with early infection, log-phases, peaking parasitaemia, and later TPs indicated for

blood and bone marrow sample collections. Necropsy endpoints (*) were planned for each species after day 14, early on in the natural overall decline in parasitaemia as observed for kra monkeys in E07 (Fig. S1) and again subsequently in E35 (Fig. S3). Bottom Panel: Schematic showing E33 experimental data including *P. knowlesi* cryopreserved sporozoite inoculations on day 0 (syringe), daily parasitaemias graphed (pink lines), and defined TPs (gold bars) and the specific days of euthanasia and necropsy endpoints (*) are indicated for each of the animals. No treatment was required.

Additional file 12: Fig. S3. E35 Experimental Design and Parasitaemia, as also similarly presented in PlasmoDB [91] to accompany E35 publicly available data. E35 includes iterative *P. knowlesi* infections in a cohort of four kra monkeys (13C33, 13C74, H13C101, H14C17) to continue to study acute and chronic infections, up to 50 days, with the later TPs 5–8 also labelled Chronic I–Chronic IV. Top Panel: Schematic of the planned (generalized) experimental design with timepoint (TP) sample collections (gold bars), *P. knowlesi* cryopreserved sporozoite inoculations at day 0 (syringe), predicted parasitaemia kinetics (pink line) with early infection, log-phases, peaking parasitaemia, and later TPs indicated for blood and bone marrow sample collections. Necropsy endpoints (*) were planned for each animal well after day 14, when the natural decline in parasitaemia was expected, as observed for the three kra monkeys with chronic infections in E07 (Fig. S1), and when parasitaemia was still undetectable. Bottom Panel: Schematic showing E35 experimental data including *P. knowlesi* cryopreserved sporozoite inoculations on day 0 (syringe), daily parasitaemias graphed (pink lines), and defined TPs (gold bars) and the specific days of euthanasia and necropsy endpoints (*) are indicated for each of the animals. No treatment was required.

Additional file 13: Fig. S4. Flow Cytometry Gating Strategy. Representative flow cytometry gating strategy for measuring erythroid lineage cells in bone marrow aspirate collected from the kra monkeys.

Additional file 14: Fig. S5. Characterization of the dynamics of RBC removal and production processes in a representative kra monkey (12C44) during a *P. knowlesi* infection. To quantify the haemodynamic processes during a *P. knowlesi* infection, a computational dynamical model was used that was previously developed to faithfully track the blood dynamics in *Plasmodium* infected monkeys [63–65]. The model was formulated as a set of discrete recursive equations, where the pools of reticulocytes, RBCs, and iRBCs were stratified into age classes. The model directly represents that reticulocytes are released from the bone marrow with a certain age and rate, circulate for a day and then mature into RBCs. Pertinent model results (lines) are superimposed on experimental data (symbols). Shown are the circulating reticulocytes (A), mature RBCs (C), and infected RBCs (F), from which the model allowed the quantification of different causes of RBC removal (D and E). The NHP RBCs normally die after about 100 days due to senescence, or on a daily basis due to “random” effects, such as shear stresses (E). During *Plasmodium* infections, some of the healthy RBCs are also infected by merozoites and destroyed when the parasites are released (parasitisation, D) or lost to a bystander effect (D). Interestingly, large numbers of RBCs were lost during the infection due to the bystander mechanism (D). The profile of RBCs (C) demonstrates that the kra monkey had severe anaemia and responded appropriately by increasing the erythropoietic output and releasing younger reticulocytes, thereby increasing the reticulocyte maturation time in circulation (B).

Acknowledgements

The authors thank John W. Barnwell for discussions, bringing knowledge of *P. knowlesi* infections and malaria to this project and the provision of cryopreserved sporozoites. Elizabeth Strobert is thanked for consultations and advice on animal protocols. E-van Dessasau is thanked for technical assistance in preparing and staining histopathological slides. The YNPRC staff are acknowledged for assistance with procedures involving NHPs, and the Emory Pediatric/Winship Flow Cytometry and Yerkes Flow Cytometry Cores are recognized for maintaining core facilities made available in this project. MaHPIC Consortium Members. MaHPIC members participating in discussions at the time of the planning, implementation, or analysis of this project include: Dave C. Anderson, Ferhat Ay, Cristiana F. A. Brito, John W. Barnwell, Megan DeBarry, Steven E. Bosinger, Jung-Ting Chien, Jinho Choi, Anuj Gupta, Chris

Begbu, Xuntian Jiang, Dean P. Jones, Nicolas Lackman, Tracey J. Lamb, Frances E.-H. Lee, Karine Gaelle Le Roche, Shuzhao Li, Esmeralda V.S. Meyer, Diego M. Moncada-Giraldo, Dan Ory, Jan Pohl, Saeid Safaei, Igñacio Sanz, Maren Smith, Gregory Tharp, ViLinh Tran, Elizabeth D. Trippe, Karan Uppal, Susanne Warrenfeltz, Tyrone Williams, Zerotti L. Woods.

Authors' contributions

Conceived and designed the experiments: MSP, CJJ, JAB, JSW, LLF, RT, JCK, AM, SG, EO, V, JBG, RJC, MRG, and members of the MaHPIC-Consortium. Performed the experiments: MSP, CJJ, JAB, JSW, MCM, CLS, LLF, WTC, JJ, SAL, SRS, AH, DM, EK. Performed data analysis: MSP, CJJ, JAB, LLF, SG, JBG. Interpreted the data analysis: MSP, CJJ, RJC, MRG and members of the MaHPIC-Consortium. Managed and led validation and quality control of datasets for clinical and telemetry results and deposited the data and metadata: MVN, JH, JDD, JCK. Generated the figures: MSP, CJJ, LLF, SG. Wrote the paper: MSP, CJJ, MRG. Provided manuscript editorial contributions: LLF, AM, SG, EO, V, RJC. All authors reviewed the manuscript. All authors read and approved the final manuscript.

Funding

This project was funded in part by the National Institute of Allergy and Infectious Diseases; National Institutes of Health, Department of Health and Human Services, which established the MaHPIC [Contract No. HHSN272201200031C; MRG], the NIH Office of Research Infrastructure Programs/OD P51OD011132, the Defense Advanced Research Program Agency and the US Army Research Office via a cooperative agreement [Contract No. W911NF16C0008; MRG], which funded the Technologies for Host Resilience-Host Acute Models of Malaria to study Experimental Resilience (THoR's HAMMER) consortium.

Availability of data and materials

All clinical and telemetry data were rigorously validated and quality controlled. The majority of data analysed here, protocols and extensive metadata are publicly available in PlasmoDB [91]: <http://plasmodb.org/plasmo/mahpic.jsp>; http://plasmodb.org/common/downloads/MaHPIC/Experiment_07/; http://plasmodb.org/common/downloads/MaHPIC/Experiment_33/; http://plasmodb.org/common/downloads/MaHPIC/Experiment_35/; Data not available through public data repositories are included as Additional file (e.g., tissue parasite counts are included in S1 Spreadsheet). Data not in public databases or supplementary files (e.g., flow cytometry data files) can be requested directly from the corresponding author.

Declarations

Ethics approval and consent to participate

All experimental, surgical, and necropsy procedures were approved by Emory's IACUC and the Animal Care and Use Review Office (ACURO) of the US Department of Defense and followed accordingly. The Emory's IACUC approval number was PROTO201700484-YER-2003344-ENTRPR-A.

Consent for publication

Not applicable.

Competing interests

The authors declare that they have no competing interests.

Author details

¹Yerkes National Primate Research Center, Emory University, Atlanta, GA, USA. ²Emory Vaccine Center, Emory University, Atlanta, GA, USA. ³Center for Vaccines and Immunology, Department of Infectious Diseases, University of Georgia, Athens, GA, USA. ⁴School of Chemical, Materials and Biomedical Engineering, University of Georgia, Athens, GA, USA. ⁵Division of Animal Resources, Yerkes National Primate Research Center, Emory University, Atlanta, GA, USA. ⁶The Wallace H. Coulter Department of Biomedical Engineering, Georgia Institute of Technology and Emory University, Atlanta, GA, USA. ⁷Institute of Bioinformatics, University of Georgia, Athens, GA, USA. ⁸Division of Pathology, Yerkes National Primate Research Center, Atlanta, GA, USA. ⁹Department of Pediatrics, Emory University School of Medicine, Atlanta, GA, USA. ¹⁰Department of Genetics, University of Georgia, Athens, GA, USA. ¹¹Center for Tropical and Emerging Global Diseases, University of Georgia, Athens, GA, USA. ¹²Division of Infectious Diseases, Department of Medicine, Emory University School of Medicine, Atlanta, GA, USA. ¹³Department

of Pathology and Laboratory Medicine, Emory School of Medicine, Atlanta, GA, USA. ¹⁴Department of Mathematics, University of Georgia, Athens, GA, USA. ¹⁵Present Address: Emory University School of Medicine, Atlanta, GA, USA. ¹⁶Present Address: Center for Vaccines and Immunology, Department of Infectious Diseases, College of Veterinary Medicine, University of Georgia, Athens, GA, USA. ¹⁷Present Address: Eli Lilly and Company, Indianapolis, IN, USA. ¹⁸Present Address: College of Veterinary Medicine, University of Georgia, Athens, GA, USA. ¹⁹Present Address: Division of Pulmonary, Critical Care, and Sleep Medicine, Department of Medicine, College of Medicine, University of Florida, Gainesville, FL, USA. ²⁰Present Address: Thermo Fisher Scientific, South San Francisco, CA, USA. ²¹Present Address: Center for Tropical & Emerging Global Diseases, University of Georgia, Athens, GA, USA. ²²Present Address: The MITRE Corporation, Atlanta, GA, USA. ²³Present Address: Department of Biosciences and Diagnostic Imaging, College of Veterinary Medicine, University of Georgia, Athens, GA, USA. ²⁴Center for Topical and Emerging Global Diseases, University of Georgia, Athens, GA, USA. ²⁵Present Address: Pathology, Drug Safety, and DMPK, Boehringer Ingelheim Animal Health USA, Inc., Athens, GA, USA. ²⁶Present Address: Department of Mathematics, University of Texas at San Antonio, San Antonio, TX, USA. ²⁷Present Address: Department of Biology, Wake Forest University, Winston-Salem, NC, USA.

Received: 18 June 2021 Accepted: 24 September 2021

Published online: 30 December 2021

References

- Singh B, Daneshvar C. Human infections and detection of *Plasmodium knowlesi*. *Clin Microbiol Rev*. 2013;26:165–84.
- Barber BE, Rajahram GS, Grigg MJ, William T, Anstey NM. World Malaria Report: time to acknowledge *Plasmodium knowlesi* malaria. *Malar J*. 2017;16:135.
- Davidson G, Chua TH, Cook A, Speldewinde P, Weinstein P. Defining the ecological and evolutionary drivers of *Plasmodium knowlesi* transmission within a multi-scale framework. *Malar J*. 2019;18:66.
- Singh B, Kim Sung L, Matusop A, Radhakrishnan A, Shamsul SS, Cox-Singh J, et al. A large focus of naturally acquired *Plasmodium knowlesi* infections in human beings. *Lancet*. 2004;363:1017–24.
- Cox-Singh J, Singh B. *Knowlesi* malaria: newly emergent and of public health importance? *Trends Parasitol*. 2008;24:406–10.
- Cox-Singh J, Davis TM, Lee KS, Shamsul SS, Matusop A, Ratnam S, Rahman HA, Conway DJ, Singh B. *Plasmodium knowlesi* malaria in humans is widely distributed and potentially life threatening. *Clin Infect Dis*. 2008;46:165–71.
- Cooper DJ, Rajahram GS, William T, Jelip J, Mohammad R, Benedict J, Alaza DA, Malacova E, Yeo TW, Grigg MJ, et al. *Plasmodium knowlesi* Malaria in Sabah, Malaysia, 2015–2017: ongoing increase in incidence despite near-elimination of the human-only *Plasmodium* species. *Clin Infect Dis*. 2020;70:361–7.
- Divis PCS, Hu TH, Kadir KA, Mohammad DSA, Hii KC, Daneshvar C, Conway DJ, Singh B. Efficient surveillance of *Plasmodium knowlesi* genetic subpopulations, Malaysian Borneo, 2000–2018. *Emerg Infect Dis*. 2020;26:1392–8.
- Chin AZ, Maluda MCM, Jelip J, Jeffrey MSB, Culleton R, Ahmed K. Malaria elimination in Malaysia and the rising threat of *Plasmodium knowlesi*. *J Physiol Anthropol*. 2020;39:36.
- Manin BO, Ferguson HM, Vythilingam I, Fornace K, William T, Torr SJ, Drakeley C, Chua TH. Investigating the contribution of peri-domestic transmission to risk of zoonotic malaria infection in humans. *PLoS Negl Trop Dis*. 2016;10:e0005064.
- Fornace KM, Abidin TR, Alexander N, Brock P, Grigg MJ, Murphy A, William T, Menon J, Drakeley CJ, Cox J. Association between landscape factors and spatial patterns of *Plasmodium knowlesi* infections in Sabah, Malaysia. *Emerg Infect Dis*. 2016;22:201–8.
- Fornace KM, Nuin NA, Betson M, Grigg MJ, William T, Anstey NM, Yeo TW, Cox J, Ying LT, Drakeley CJ. Asymptomatic and submicroscopic carriage of *Plasmodium knowlesi* malaria in household and community members of clinical cases in Sabah, Malaysia. *J Infect Dis*. 2016;213:784–7.
- Barber BE, William T, Dhararaj P, Anderios F, Grigg MJ, Yeo TW, Anstey NM. Epidemiology of *Plasmodium knowlesi* malaria in north-east Sabah, Malaysia: family clusters and wide age distribution. *Malar J*. 2012;11:401.
- Vythilingam I, Noorazian YM, Huat TC, Jiram AI, Yusri YM, Azahari AH, Norparina I, Noorain A, Lokmanhakim S. *Plasmodium knowlesi* in humans, macaques and mosquitoes in peninsular Malaysia. *Parasit Vectors*. 2008;1:26.
- Divis PC, Singh B, Anderios F, Hisam S, Matusop A, Kocken CH, Assefa SA, Duffy CW, Conway DJ. Admixture in humans of two divergent *Plasmodium knowlesi* populations associated with different macaque host species. *PLoS Pathog*. 2015;11:e1004888.
- Fungfuang W, Udom C, Tongthainan D, Kadir KA, Singh B. Malaria parasites in macaques in Thailand: stump-tailed macaques (*Macaca arctoides*) are new natural hosts for *Plasmodium knowlesi*, *Plasmodium inui*, *Plasmodium coatneyi* and *Plasmodium fieldi*. *Malar J*. 2020;19:350.
- Lee KS, Divis PC, Zakaria SK, Matusop A, Julin RA, Conway DJ, Cox-Singh J, Singh B. *Plasmodium knowlesi*: reservoir hosts and tracking the emergence in humans and macaques. *PLoS Pathog*. 2011;7:e1002015.
- Ta TH, Hisam S, Lanza M, Jiram AI, Ismail N, Rubio JM. First case of a naturally acquired human infection with *Plasmodium cynomolgi*. *Malar J*. 2014;13:68.
- Imwong M, Madmanee W, Suwannasin K, Kunasol C, Peto TJ, Tripura R, von Seidlein L, Nguon C, Davoeung C, Day NPJ, et al. Asymptomatic natural human infections with the simian malaria parasites *Plasmodium cynomolgi* and *Plasmodium knowlesi*. *J Infect Dis*. 2018;219:695–702.
- Singh B, Kadir KA, Hu TH, Raja TN, Mohamad DS, Lin LW, Hii KC. Naturally acquired human infections with the simian malaria parasite, *Plasmodium cynomolgi*, in Sarawak, Malaysian Borneo. *Int J Infect Dis*. 2018;73:68.
- Raja TN, Hu TH, Kadir KA, Mohamad DSA, Rosli N, Wong LL, Hii KC, Simon Divis PC, Singh B. Naturally acquired human *Plasmodium cynomolgi* and *P. knowlesi* infections, Malaysian Borneo. *Emerg Infect Dis*. 2020;26:1801–9.
- Chin W, Contacos PG, Coatney GR, Kimball HR. A naturally acquired quotidian-type malaria in man transferable to monkeys. *Science*. 1965;149:865.
- Cox-Singh J, Hiu J, Lucas SB, Divis PC, Zulkarnaen M, Chandran P, Wong KT, Adem P, Zaki SR, Singh B, Krishna S. Severe malaria - a case of fatal *Plasmodium knowlesi* infection with post-mortem findings: a case report. *Malar J*. 2010;9:10.
- Daneshvar C, Davis TM, Cox-Singh J, Rafaeel MZ, Zakaria SK, Divis PC, Singh B. Clinical and laboratory features of human *Plasmodium knowlesi* infection. *Clin Infect Dis*. 2009;49:852–60.
- Noordin NR, Lee PY, Mohd Bukhari FD, Fong MY, Abdul Hamid MH, Jelip J, Mudin RN, Lau YL. Prevalence of asymptomatic and/or low-density malaria infection among high-risk groups in Peninsular Malaysia. *Am J Trop Med Hyg*. 2020;103:1107–10.
- Imwong M, Madmanee W, Suwannasin K, Kunasol C, Peto TJ, Tripura R, von Seidlein L, Nguon C, Davoeung C, Day NPJ, et al. Asymptomatic natural human infections with the simian malaria parasites *Plasmodium cynomolgi* and *Plasmodium knowlesi*. *J Infect Dis*. 2019;219:695–702.
- Jiram AI, Hisam S, Reuben H, Husin SZ, Roslan A, Ismail WRW. Submicroscopic evidence of the simian malaria parasite, *Plasmodium knowlesi*, in an Orang Asli community. *Southeast Asian J Trop Med Public Health*. 2016;47:591–9.
- Jiram AI, Ooi CH, Rubio JM, Hisam S, Kaman G, Sukor NM, Artic MM, Ismail NP, Alias NW. Evidence of asymptomatic submicroscopic malaria in low transmission areas in Belaga district, Kapit division, Sarawak, Malaysia. *Malar J*. 2019;18:156.
- Lubis IND, Wijaya H, Lubis M, Lubis CP, Divis PCS, Beshir KB, Sutherland CJ. Contribution of *Plasmodium knowlesi* to multispecies human malaria infections in North Sumatera, Indonesia. *J Infect Dis*. 2017;215:1148–55.
- Barber BE, William T, Grigg MJ, Menon J, Auburn S, Marfurt J, Anstey NM, Yeo TW. A prospective comparative study of *knowlesi*, *falciparum*, and *vivax* malaria in Sabah, Malaysia: high proportion with severe disease from *Plasmodium knowlesi* and *Plasmodium vivax* but no mortality with early referral and artesunate therapy. *Clin Infect Dis*. 2013;56:383–97.
- Barber BE, William T, Jikal M, Jilip J, Dhararaj P, Menon J, Yeo TW, Anstey NM. *Plasmodium knowlesi* malaria in children. *Emerg Infect Dis*. 2011;17:814–20.
- Grigg MJ, William T, Barber BE, Rajahram GS, Menon J, Schimann E, Piera K, Wilkes CS, Patel K, Chandna A, et al. Age-related clinical spectrum of *Plasmodium knowlesi* malaria and predictors of severity. *Clin Infect Dis*. 2018;67:350–9.
- Rajahram GS, Barber BE, William T, Grigg MJ, Menon J, Yeo TW, Anstey NM. Falling *Plasmodium knowlesi* malaria death rate among adults despite rising incidence, Sabah, Malaysia, 2010–2014. *Emerg Infect Dis*. 2016;22:41–8.
- Rajahram GS, Cooper DJ, William T, Grigg MJ, Anstey NM, Barber BE. Deaths from *Plasmodium knowlesi* malaria: case series and systematic review. *Clin Infect Dis*. 2019;69:1703–11.

35. William T, Menon J, Rajahram G, Chan L, Ma G, Donaldson S, Khoo S, Frederick C, Jelip J, Anstey NM, Yeo TW. Severe *Plasmodium knowlesi* malaria in a tertiary care hospital, Sabah, Malaysia. *Emerg Infect Dis*. 2011;17:1248–55.
36. Daneshvar C, William T, Davis TME. Clinical features and management of *Plasmodium knowlesi* infections in humans. *Parasitology*. 2018;145:18–31.
37. World Health Organization. Severe malaria. *Trop Med Int Health*. 2014;19:7–131.
38. Barber BE, Grigg MJ, William T, Yeo TW, Anstey NM. The treatment of *Plasmodium knowlesi* malaria. *Trends Parasitol*. 2017;33:242–53.
39. Rajahram GS, Cooper DJ, William T, Grigg MJ, Anstey NM, Barber BE. Deaths from *Plasmodium knowlesi* malaria: case series and systematic review. *Clin Infect Dis*. 2019;69(10):1703–11.
40. Collins WE. *Plasmodium knowlesi*: a malaria parasite of monkeys and humans. *Annu Rev Entomol*. 2012;57:107–21.
41. Pasini EM, Zeeman AM, Voorberg Van der Wel A, Kocken CH. *Plasmodium knowlesi*: a relevant, versatile experimental malaria model. *Parasitology*. 2018;145:56–70.
42. Galinski MR, Lapp SA, Peterson MS, Ay F, Joyner CJ, Le Roch KG, Fonseca LL, Voit EO. *Plasmodium knowlesi*: a superb in vivo nonhuman primate model of antigenic variation in malaria. *Parasitology*. 2018;145:85–100.
43. Knowles R, Gupta BMD. A study of monkey-malaria, and its experimental transmission to man. *Ind Med Gaz*. 1932;67:301–20.
44. Coatney GR, Collins WE, Warren M, Contacos PG. The Primate Malaria. Washington: DC. U.S Department of Health, Education and Welfare; 1971.
45. Coatney GR, Collins WE, Warren M, Contacos PG. The Primate Malaria, e-book [original book published in 1971] pp. 381. Atlanta, GA, USA: Division of Parasitic Diseases, Centers for Disease Control and Protection; 2003:381.
46. Brown KN, Brown IN. Immunity to malaria: antigenic variation in chronic infections of *Plasmodium knowlesi*. *Nature*. 1965;208:1286–8.
47. Butcher GA, Cohen S. Antigenic variation and protective immunity in *Plasmodium knowlesi* malaria. *Immunology*. 1972;23:503–21.
48. Barnwell JW, Howard RJ, Coon HG, Miller LH. Splenic requirement for antigenic variation and expression of the variant antigen on the erythrocyte membrane in cloned *Plasmodium knowlesi* malaria. *Infect Immun*. 1983;40:985–94.
49. Miller LH, Fremount HN, Luse SA. Deep vascular schizogony of *Plasmodium knowlesi* in *Macaca mulatta*. Distribution in organs and ultrastructure of parasitized red cells. *Am J Trop Med Hyg*. 1971;20:816–24.
50. Spangler WL, Gribble D, Abildgaard C, Harrison J. *Plasmodium knowlesi* malaria in the Rhesus monkey. *Vet Pathol*. 1978;15:83–91.
51. Butcher GA, Mitchell GH, Cohen S. *Plasmodium knowlesi* infections in a small number of non-immune natural hosts (*Macaca fascicularis*) and in rhesus monkeys (*M. mulatta*). *Trans R Soc Trop Med Hyg*. 2010;104:75–7.
52. Butcher GA. Models for malaria: nature knows best. *Parasitol Today*. 1996;12:378–82.
53. Anderios F, Noorain A, Vythilingam I. In vivo study of human *Plasmodium knowlesi* in *Macaca fascicularis*. *Exp Parasitol*. 2010;124:181–9.
54. Barber BE, Russell B, Grigg MJ, Zhang R, William T, Amir A, Lau YL, Chatfield MD, Dondorp AM, Anstey NM, Yeo TW. Reduced red blood cell deformability in *Plasmodium knowlesi* malaria. *Blood Adv*. 2018;2:433–43.
55. Gupta A, Styczynski MP, Galinski MR, Voit EO, Fonseca LL. Dramatic transcriptional differences in *Macaca mulatta* and *Macaca fascicularis* with *Plasmodium knowlesi* infections. *Sci Reports* 2021. In Press.
56. Percie du Sert N, Hurst V, Ahluwalia A, Alam S, Avey MT, Baker M, Browne WJ, Clark A, Cuthill IC, Dirnagl U, et al. The ARRIVE guidelines 2.0: updated guidelines for reporting animal research. *PLoS Biol*. 2020;18:e3000410.
57. Lapp SA, Geraldo JA, Chien JT, Ay F, Pakala SB, Batugedara G, Humphrey J, MaHPIC-Consortium, De Barry JD, Le Roch KG, et al. PacBio assembly of a *Plasmodium knowlesi* genome sequence with Hi-C correction and manual annotation of the SICAv gene family. *Parasitology*. 2018;145:71–84.
58. Joyner CJ, Moreno A, Meyer EVS, Cabrera-Mora M, MaHPIC-Consortium, Kissinger JC, Barnwell JW, Galinski MR. *Plasmodium cynomolgi* infections in rhesus macaques display clinical and parasitological features pertinent to modelling vivax malaria pathology and relapse infections. *Malar J*. 2016;15:1–18.
59. Earle WC, Perez M. Enumeration of parasites in the blood of malarial patients. *J Lab Clin Med*. 1932;17:1124–30.
60. Fonseca LL, Joyner CJ, MaHPIC-Consortium, Galinski MR, Voit EO. A model of *Plasmodium vivax* concealment based on *Plasmodium cynomolgi* infections in *Macaca mulatta*. *Malar J*. 2017;16:1–16.
61. Peterson MS, Joyner CJ, Cordy RJ, Salinas JL, Machiah D, Lapp SA, MaHPIC-Consortium, Meyer VS, Gumber S, Galinski MR. *Plasmodium vivax* parasite load is associated with histopathology in *Saimiri boliviensis* with findings comparable to *P. vivax* pathogenesis in humans. *Open Forum Infect Dis*. 2019;6:1–9.
62. Tang Y, Joyner CJ, Cabrera-Mora M, Lapp SA, Nural MV, Pakala SB, DeBarry JD, Soderberg S, MaHPIC-Consortium, Kissinger JC, et al. Integrative analysis associates monocytes with insufficient erythropoiesis during acute *Plasmodium cynomolgi* malaria in rhesus macaques. *Malar J*. 2017;16:1–16.
63. Fonseca LL, Alezi HS, Moreno A, Barnwell JW, Galinski MR, Voit EO. Quantifying the removal of red blood cells in *Macaca mulatta* during a *Plasmodium coatneyi* infection. *Malar J*. 2016;15:410.
64. Fonseca LL, Joyner CJ, Saney CL, MaHPIC-Consortium, Moreno A, Barnwell JW, Galinski MR, Voit EO. Analysis of erythrocyte dynamics in rhesus macaque monkeys during infection with *Plasmodium cynomolgi*. *Malar J*. 2018;17:410.
65. Fonseca LL, Voit EO. Comparison of mathematical frameworks for modeling erythropoiesis in the context of malaria infection. *Math Biosci*. 2015;270:224–36.
66. Moreno A, Cabrera-Mora M, Garcia A, Orkin J, Strobert E, Barnwell JW, Galinski MR. *Plasmodium coatneyi* in rhesus macaques replicates the multisystemic dysfunction of severe malaria in humans. *Infect Imm*. 2013;81:1889–904.
67. Mitchell GH, Butcher GA, Cohen S. Isolation of blood-stage merozoites from *Plasmodium knowlesi* malaria. *Int J Parasitol*. 1973;3:443–5.
68. Cordy RJ, Patrapuvich R, Lili LN, Cabrera-Mora M, Chien J-T, Sharp GK, Khadka M, Meyer EVS, Lapp SA, Joyner CJ, et al. Distinct amino acid and lipid perturbations characterize acute versus chronic malaria. *JCI Insight*. 2019;4:1–21.
69. Lacerda MV, Mourao MP, Coelho HC, Santos JB. Thrombocytopenia in malaria: who cares? *Mem Inst Oswaldo Cruz*. 2011;106(Suppl 1):52–63.
70. Perkins DJ, Were T, Davenport GC, Kempalah P, Hittner JB, Ong'echa JM. Severe malarial anemia: innate immunity and pathogenesis. *Int J Biol Sci*. 2011;7:1427–42.
71. Lamikanra AA, Brown D, Potocnik A, Casals-Pascual C, Langhorne J, Roberts DJ. Malarial anemia: of mice and men. *Blood*. 2007;110:18–28.
72. Chang KH, Tam M, Stevenson MM. Inappropriately low reticulocytosis in severe malarial anemia correlates with suppression in the development of late erythroid precursors. *Blood*. 2004;103:3727–35.
73. Thawani N, Tam M, Bellemare MJ, Bohle DS, Olivier M, de Souza JB, Stevenson MM. *Plasmodium* products contribute to severe malarial anemia by inhibiting erythropoietin-induced proliferation of erythroid precursors. *J Infect Dis*. 2014;209:140–9.
74. Kho S, Barber BE, Johar E, Andries B, Poespoprodjo JR, Kenangalem E, Piera KA, Ehmann A, Price RN, William T, et al. Platelets kill circulating parasites of all major *Plasmodium* species in human malaria. *Blood*. 2018;132:1332–44.
75. Raja AI, Brickley EB, Taaffe J, Ton T, Zhao Z, Bock KW, Orr-Gonzalez S, Thomas ML 3rd, Lambert LE, Moore IN, Duffy PE. A primate model of severe malarial anaemia: a comparative pathogenesis study. *Sci Rep*. 2019;9:18965.
76. White NJ. Anaemia and malaria. *Malar J*. 2018;17:371.
77. Collins WE, Jeffery GM, Roberts JM. A retrospective examination of anemia during infection of humans with *Plasmodium vivax*. *Am J Trop Med Hyg*. 2003;68:410–2.
78. Jakeman GN, Saul A, Hogarth WL, Collins WE. Anaemia of acute malaria infections in non-immune patients primarily results from destruction of uninfected erythrocytes. *Parasitology*. 1999;119(Pt 2):127–33.
79. Looareesuwan S, Merry AH, Phillips RE, Pleehachinda R, Wattanagoon Y, Ho M, Charoenlarp P, Warrell DA, Weatherall DJ. Reduced erythrocyte survival following clearance of malarial parasitaemia in Thai patients. *Br J Haematol*. 1987;67:473–8.
80. Knisely MH, Stratman-Thomas WK, et al. Knowlesi malaria in monkeys; microscopic pathological circulatory physiology of rhesus monkeys during acute *Plasmodium knowlesi* malaria. *J Natl Malar Soc*. 1945;4:285–300.
81. Miller LH, Usami S, Chien S. Alteration in the rheologic properties of *Plasmodium knowlesi*-infected red cells. A possible mechanism for capillary obstruction. *J Clin Invest*. 1971;50:1451–5.
82. Rigdon RH, Stratman Thomas WK. A study of the pathological lesions in *P. knowlesi* infection in *M. rhesus* monkeys. *Amer J Trop Med Hyg*. 1942;51–22:329–39.
83. Joyner CJ, MaHPIC-Consortium, Wood JS, Moreno A, Garcia A, Galinski MR. Case report: severe and complicated *cynomolgi* malaria in a rhesus macaque resulted in similar histopathological changes as those seen in human malaria. *Am J Trop Med Hyg*. 2017;97:548–55.
84. Moreno A, Garcia A, Cabrera-Mora M, Strobert E, Galinski MR. Disseminated intravascular coagulation complicated by peripheral gangrene in a rhesus

- macaque (*Macaca mulatta*) experimentally infected with *Plasmodium coatneyi*. *Am J Trop Med Hyg.* 2007;76:648–54.
85. Lombardini ED, Gettayacamin M, Turner GD, Brown AE. A review of *Plasmodium coatneyi*-macaque models of severe malaria. *Vet Pathol.* 2015;52:998–1011.
 86. Dankwa S, Lim C, Bei AK, Jiang RH, Abshire JR, Patel SD, Goldberg JM, Moreno Y, Kono M, Niles JC, Duraisingh MT. Ancient human sialic acid variant restricts an emerging zoonotic malaria parasite. *Nat Commun.* 2016;7:11187.
 87. Napier LE, Campbell HGM. Observations on a *Plasmodium* infection which causes haemoglobinuria in certain species of monkey. *Ind Med Gaz.* 1932;67:246–9.
 88. Schmidt LH, Fradkin R, Harrison J, Rossan RN. Differences in the virulence of *Plasmodium knowlesi* for *Macaca irus (fascicularis)* of Philippine and Malayan origins. *Am J Trop Med Hyg.* 1977;26:612–22.
 89. Collins WE, Skinner JC, Broderson JR, Filipski VK, Morris CM, Stanfill PS, Warren M. Susceptibility of *Macaca fascicularis* monkeys from Mauritius to different species of *Plasmodium*. *J Parasitol.* 1992;78:505–11.
 90. Gupta A, Galinski MR, Voit EO. Dynamic control balancing cell proliferation and inflammation is crucial for an effective immune response to malaria. *Front Mol Biosci.* 2021 (in press).
 91. Aurrecoechea C, Brestelli J, Brunk BP, Dommer J, Fischer S, Gajria B, Gao X, Gingle A, Grant G, Harb OS, et al. PlasmoDB: a functional genomic database for malaria parasites. *Nucleic Acids Res.* 2009;37:D539–543.
 92. DeBarry JD, Kissinger JC, Nural MV, Pakala SB, Humphrey JC, Meyer EVS, Cordy RJ, Cabrera-Mora M, Trippe ED, Aguilar JB, et al. Practical recommendations for supporting a systems biology cyberinfrastructure. *Data Sci J.* 2020;19:1–12.

Publisher's Note

Springer Nature remains neutral with regard to jurisdictional claims in published maps and institutional affiliations.

Ready to submit your research? Choose BMC and benefit from:

- fast, convenient online submission
- thorough peer review by experienced researchers in your field
- rapid publication on acceptance
- support for research data, including large and complex data types
- gold Open Access which fosters wider collaboration and increased citations
- maximum visibility for your research: over 100M website views per year

At BMC, research is always in progress.

Learn more biomedcentral.com/submissions

